# General Disclaimer

## One or more of the Following Statements may affect this Document

- This document has been reproduced from the best copy furnished by the organizational source. It is being released in the interest of making available as much information as possible.

- This document may contain data, which exceeds the sheet parameters. It was furnished in this condition by the organizational source and is the best copy available.

- This document may contain tone-on-tone or color graphs, charts and/or pictures, which have been reproduced in black and white.

- This document is paginated as submitted by the original source.

- Portions of this document are not fully legible due to the historical nature of some of the material. However, it is the best reproduction available from the original submission.
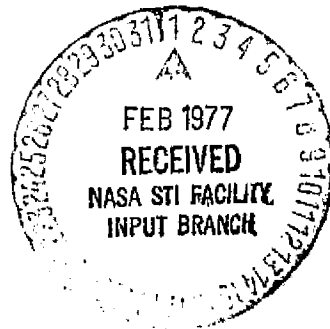
# NASA TECHNICAL MEMORANDUM

NASA TM X-73355

# A PERFORMANCE EVALUATION OF VARIOUS COATINGS, SUBSTRATE MATERIALS, AND SOLAR COLLECTOR SYSTEMS

By F. J. Dolan
Materials and Processes Laboratory

FEB 1977
RECEIVED
NASA STI FACILITY
INPUT BRANCH

September 1976

**NASA**

*George C. Marshall Space Flight Center*

*Marshall Space Flight Center, Alabama*

| 1. REPORT NO. NASA TM X-73355 | 2. GOVERNMENT ACCESSION NO. | 3. RECIPIENT'S CATALOG NO. |
|---|---|---|
| 4. TITLE AND SUBTITLE A Performance Evaluation of Various Coatings, Substrate Materials, and Solar Collector Systems | | 5. REPORT DATE September 1976 |
| | | 6. PERFORMING ORGANIZATION CODE |
| 7. AUTHOR(S) F. J. Dolan | | 8. PERFORMING ORGANIZATION REPORT # |
| 9. PERFORMING ORGANIZATION NAME AND ADDRESS George C. Marshall Space Flight Center Marshall Space Flight Center, Alabama 35812 | | 10. WORK UNIT, NO. |
| | | 11. CONTRACT OR GRANT NO. |
| | | 13. TYPE OF REPORT & PERIOD COVERED |
| 12. SPONSORING AGENCY NAME AND ADDRESS National Aeronautics and Space Administration Washington, D.C. 20546 | | Technical Memorandum |
| | | 14. SPONSORING AGENCY CODE |

15. SUPPLEMENTARY NOTES

Prepared by Materials and Processes Laboratory, Science and Engineering

16. ABSTRACT

The energy crisis and a national concern for conserving energy resources have caused Congress to establish the Energy Research and Development Administration (ERDA). The ERDA has enlisted the Marshall Space Flight Center to perform certain aspects of a research and development program directed toward demonstrating the practical use of solar heating within 3 years and combined solar heating and cooling within 5 years. In conjunction with this solar research and development effort, it became apparent that a method of testing and evaluating solar panel coatings and designs and solar collector subsystems was necessary to quickly and easily make comparisons between representative candidate samples of each. An experimental apparatus was constructed and utilized in conjunction with both a solar simulator and actual sunlight to test and evaluate various solar panel coatings, panel designs, and scaled-down collector subsystems. Data were taken by an automatic digital data acquisition system and reduced and printed by a computer system. The solar collector test setup, data acquisition system, and data reduction and printout systems were considered to have operated very satisfactorily. Test data indicated that there is a practical or useful limit in scaling down beyond which scaled-down testing cannot produce results comparable to results of larger scale tests. Test data are presented herein as are schematics and pictures of test equipment and test hardware.

| 17. KEY WORDS | | 18. DISTRIBUTION STATEMENT Unclassified — Unlimited | |
|---|---|---|---|
| 19. SECURITY CLASSIF. (of this report) Unclassified | 20. SECURITY CLASSIF. (of this page) Unclassified | 21. NO. OF PAGES 85 | 22. PRICE NTIS |

# ACKNOWLEDGMENTS

# TABLE OF CONTENTS ·

iii

# LIST OF ILLUSTRATIONS

iv

# LIST OF ILLUSTRATIONS (Continued)

# LIST OF ILLUSTRATIONS (Concluded)

# LIST OF TABLES

# A PERFORMANCE EVALUATION OF VARIOUS COATINGS, SUBSTRATE MATERIALS, AND SOLAR COLLECTOR SYSTEMS

## SUMMARY

A portable recirculating water flow and temperature control device was constructed and utilized in conjunction with both a solar simulator and actual sunlight to test and evaluate several solar collector panel coatings, panel designs, and scaled-down collector subsystems. Tests were performed on two different sizes of vacuum insulated solar collectors including tests of two different substrate materials and five different coating/substrate combinations. Tests were also performed on nine different coatings/panel designs utilizing an insulated box solar collector (flat plate collector).

Tests were made primarily with a solar simulator; however, the larger of the two vacuum insulated collectors and one of the insulated box solar collector configurations were tested outside in direct sunlight. In addition to tests in direct sunlight, other tests were made to study the effect of vacuum insulation on stagnation temperature and heat gain, the effect of flow rate and inlet temperature on heat gain, and the effect of reflectors on heat gain.

The test program is not complete and additional tests are planned, but based on the data in this report, it appears that an insulated box (flat plate) collector similar to the one tested with a low cost nonselective coating would be satisfactory for residential and commercial space heating and service hot water systems.

The vacuum insulated solar collectors tested to date have not been optimized; considerable improvement should be possible. Test data indicate that optimized units with concentrating reflectors should permit operating temperatures high enough for use in absorption air conditioning systems.

# I.  INTRODUCTION

As a result of the rising costs and rapid depletion of the nation's fossil fuel resources, the uncertainties of foreign energy supplies and costs, the problems associated with electric power generation from nuclear sources, and the probable impending depletion of national natural nuclear material resources, increased industry and governmental concern has been voiced relative to conserving our remaining natural energy resources.

As a result Congress took action to establish the Energy Research and Development Administration (ERDA), an organization with responsibilities for organizing and controlling federal efforts in the energy research and development area.  Further, Congress initiated the Solar Heating and Cooling Demonstration Act of 1974 (Public Law 93-409) which provides for demonstration of the practical use of solar heating technology within 3 years and of combined heating and cooling technology within 5 years.

As an outgrowth of this national concern for conserving energy resources, the National Aeronautics and Space Administration (NASA) and the Marshall Space Flight Center (MSFC) have become interested and active in solar heating and cooling research.  A large percentage of this effort has been directed toward solar collector subsystems, solar panels, and solar panel coating research and development.  This status report presents the findings, conclusions, and recommendations resulting from a portion of the MSFC solar collector coatings and solar collector subsystems test programs.  Further testing is planned on additional coatings and solar collector subsystem designs.

# II.  TESTING RATIONALE

The energy crisis and the need to conserve energy have caused increased interest in utilizing solar energy as an alternate source for residential and commercial heating and cooling.  Along with this increased interest has come increased testing of solar collectors and entire systems.  Primarily testing has been performed on full scale collectors with much of this work done outside in sunlight.  This full scale outdoor testing has led to the realization that test progress is very slow and that test data are difficult, if not impossible, to

correlate and compare because of the variability and uncontrollability of weather conditions. Because of these difficulties, the realization that there are countless numbers of combinations of solar collector coatings and solar collector plate and collector subsystem designs which require test and comparison, and the need to perform these tests and correlations as rapidly as possible, the consideration for utilizing solar simulators and scaled-down collectors was proposed by MSFC Materials and Processes Laboratory management.

The utilization of solar simulators would permit tests to be accomplished at a constant solar radiation intensity and angle with respect to the solar collector regardless of weather conditions or time of day. The use of solar simulators and scaled-down solar collector subsystems would permit the test and evaluation of each coating, solar panel, and/or each solar collector subsystem under identical test conditions such that meaningful comparisons could be made and test data could be repeated or verified as necessary, as well as permit a savings in material and manufacturing costs. Perhaps most importantly, however, this would permit the complete evaluation/characterization of a solar collector coating, solar panel, or solar collector subsystem in less than one standard 40 h work week regardless of the weather, season, or time of day.

Scaled-down tests were proposed because of solar simulator beam size limitations and because of material, manufacturing, and test savings. Plans were also discussed to test limited larger size solar collector subsystems to determine scaling factors and their effects and to perform limited tests outside in actual sunlight for solar simulation comparison and verification purposes.

There was concern that the available xenon tube type solar simulators would not duplicate the Sun from a spectral energy standpoint and that heat gain data from those sources would not correlate well with actual sunlight data. For this reason, limited backup comparative tests in actual sunlight were proposed. Energy spectrum measurements of both the solar simulator used and actual sunlight were also planned.

## A. Test System

The primary objectives of this program were to construct a workable solar collector subsystem test setup, to characterize and compare the heat gain performance of representative solar collector coatings and scaled-down solar collector subsystems utilizing a solar simulator, to compare solar simulator test data with that taken outside in sunlight, and to compare scaled-down solar collector subsystem test data with that of a larger solar collector of the same design.

The solar collector subsystem test setup design was driven by the desired test sequence/procedure and data requirements but was tempered by the availability of material and equipment. Basically it was intended that the test setup and instrumentation/data system permit the following types of tests to be accomplished:

1. Dry Stagnation — The solar collector plate temperature is recorded as a function of time while the solar collector subsystem is exposed to some form of solar type radiation without coolant in the water passages. It is also desirable to measure and/or record the solar type radiation intensity, particularly during sunlight tests.

2. Heat Gain as a Function of Coolant Flow Rate — This was not an individual test, rather it was a series of tests producing data for use in curve plotting. The individual data points were obtained by measuring and recording the temperatures at the inlet and outlet of the solar collector with water flowing through it at a measured and recorded constant flow rate, while the solar collector was subjected to a known constant radiation from the solar simulator. For each individual data point all variables were held as constant as possible. The entire series of tests was run with a constant inlet temperature. Each successive data point was run at a slightly higher constant flow rate such that the curve could be plotted; all other parameters were held constant.

3. Heat Gain as a Function of Inlet Temperature — This again was not an individual test, but was a series of tests. The data from the test series were used to plot the curve. The individual data points were obtained by measuring and recording the temperatures at the inlet and outlet of the solar collector with water flowing through it at a measured and recorded constant flow rate, while the solar collector was subjected to a known constant radiation from the solar simulator. For each individual data point all variables, flow rate, inlet temperature, and solar intensity, were held as constant as possible. Each successive data point was run at a higher constant inlet temperature such that the curve could be plotted; all other parameters were held constant.

4. Other Tests — All other tests were merely variations of the two basic tests described.

The solar collector test device which was used for these tests is shown schematically in Figure 1 and pictorially in Figures 2, 3, and 4. Water from the reservoir floods the suction of the centrifugal pump via the force of gravity; the pump picks it up and provides the pressure required to force the water

4
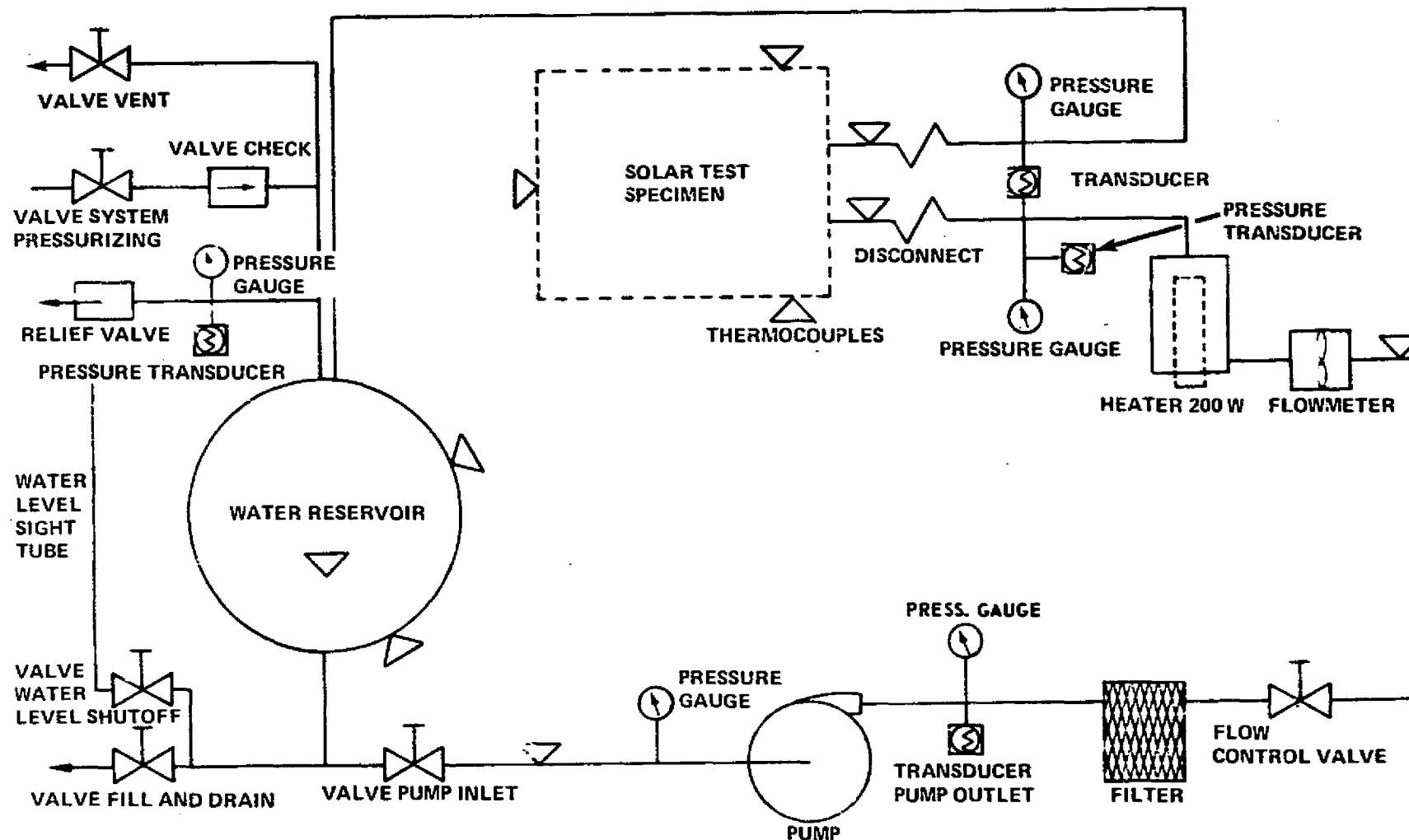
Figure 1.  Solar collector test device schematic.

VALVE VENT

VALVE CHECK

VALVE SYSTEM
PRESSURIZING

PRESSURE
GAUGE

RELIEF VALVE

PRESSURE TRANSDUCER

WATER
LEVEL
SIGHT
TUBE

WATER RESERVOIR

VALVE
WATER
LEVEL SHUTOFF

VALVE FILL AND DRAIN

VALVE PUMP INLET

PRESSURE
GAUGE

PUMP

PRESS. GAUGE

TRANSDUCER
PUMP OUTLET

FILTER

FLOW
CONTROL VALVE

SOLAR TEST
SPECIMEN

THERMOCOUPLES

DISCONNECT

PRESSURE
GAUGE

TRANSDUCER

PRESSURE
TRANSDUCER

PRESSURE GAUGE

HEATER 200 W    FLOWMETER

Figure 2. Solar collector test setup.

SOLAR SIMULATOR

THERMOCOUPLE VACUUM GAUGE

IONIZATION VACUUM GAUGE

ROUGHING VACUUM PUMP

LN$_2$ COLD TRAP
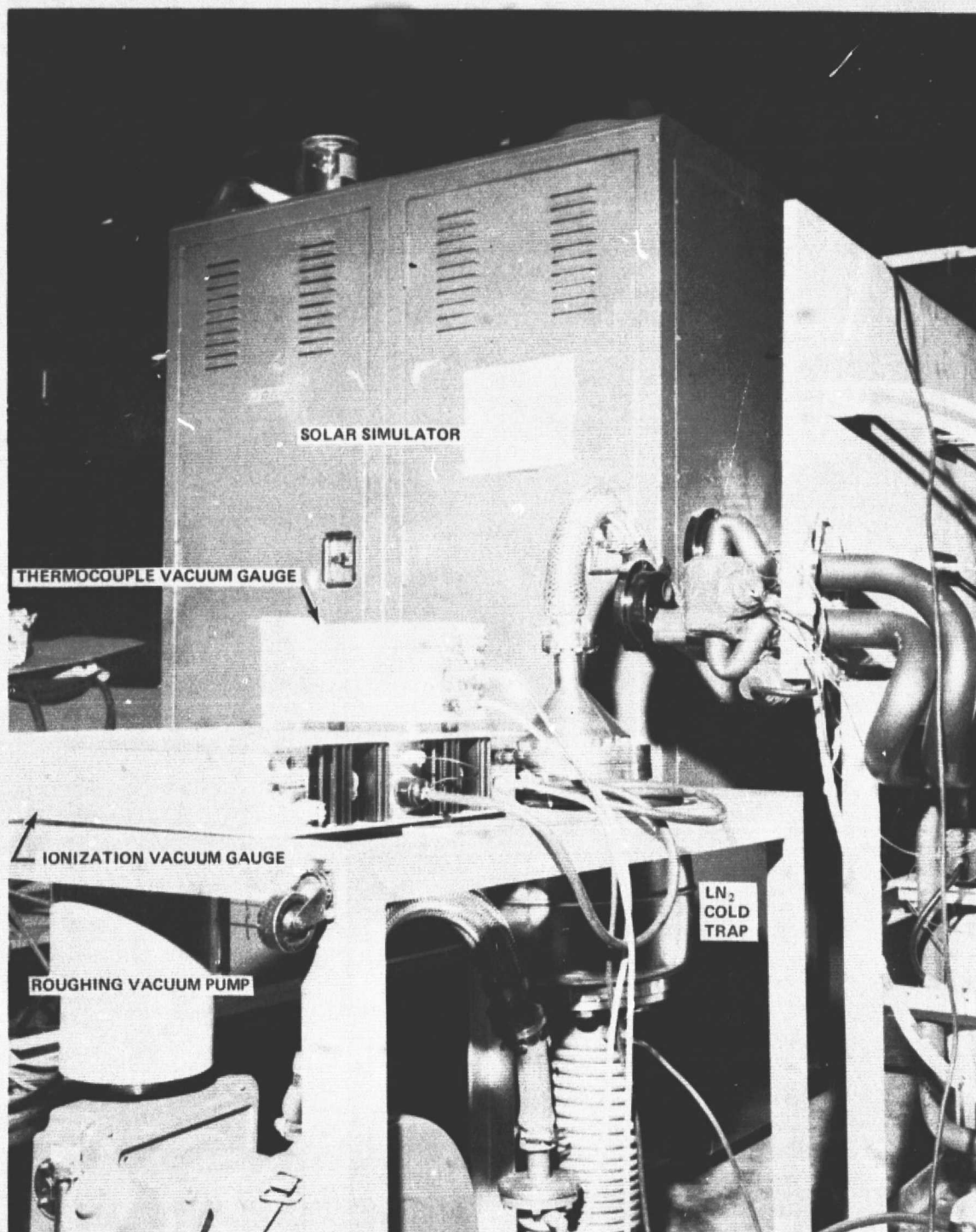
Figure 3.  Solar collector test setup.
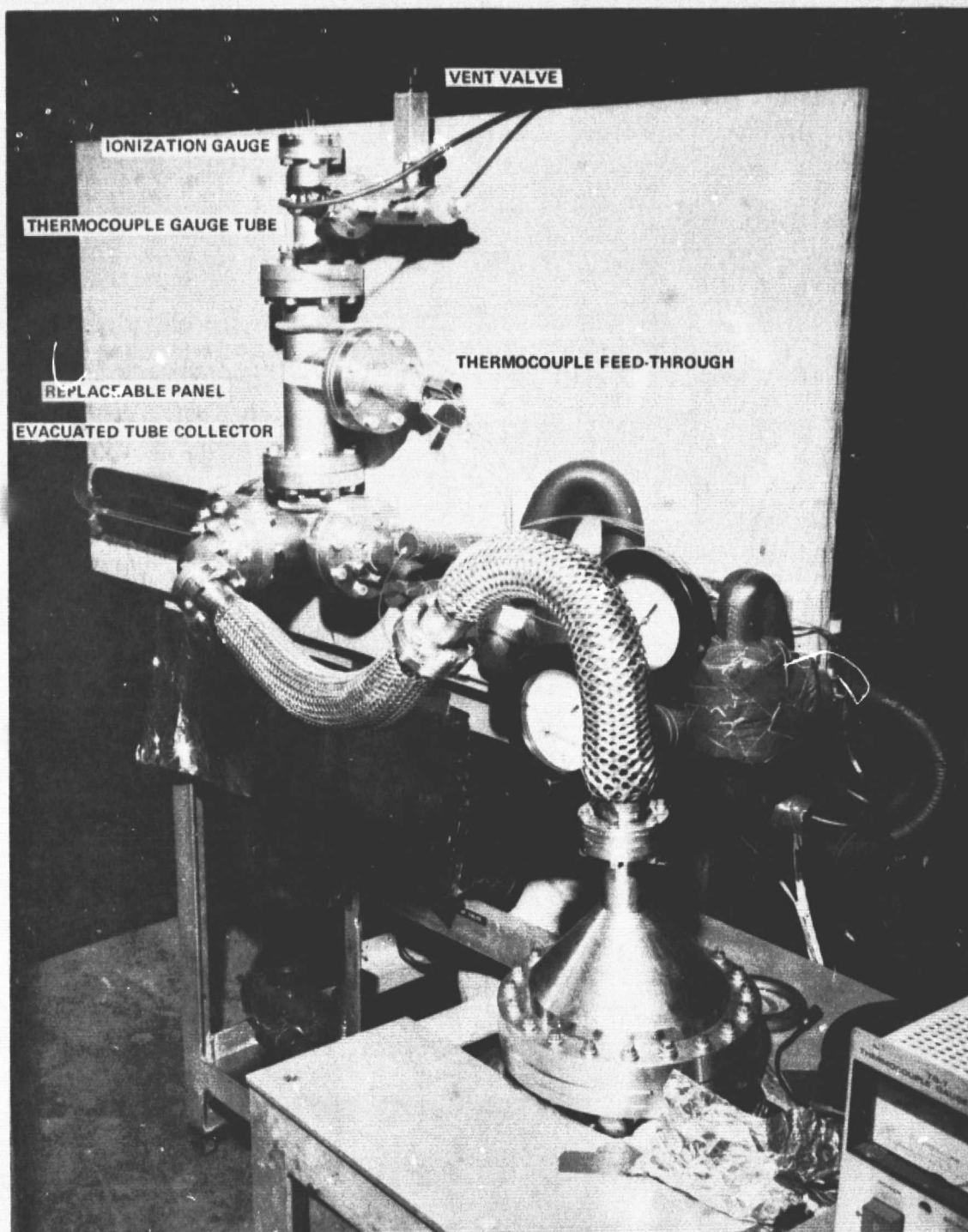
Figure 4.  Solar collector test setup with replaceable panel
evacuated tube collector mounted.

through a filter and a water flow control valve, across a thermocouple, through
a flowmeter and a heater, and then through the solar collector test specimen and
back to the reservoir in a closed-loop fashion (Fig. 1). The two thermocouples
at the inlet and outlet to the solar collector test specimen were placed as close
to the test specimen as possible and were centered in the water flow path for
best average temperature sensing.

## B. Test System Operation

The system was constructed such that it could be pressurized to prevent
boiling and allow operation above 100°C; however, all tests to date have been
made unpressurized, with the vent valve open, the water level shut off, the
pump inlet valves open, and the fill and drain valve closed. With the reservoir
one-half to three-fourths full and the pump running, the water flow control valve
was adjusted for the desired flow rate while observing the water flowmeter output
which was displayed on the digital counter (Fig. 5). The heater (Fig. 1) was
used to control the water temperature at the inlet to the solar collector test
specimen. The heater output was controlled with the Variac mounted directly
above the pump drive motor (Fig. 2). The solar simulator output was control-
lable, and it was set utilizing the pyrheliometer and a digital multimeter. The
digital multimeter was used to read the pyrheliometer output which was in
millivolts dc. On tests of the vacuum tube collector, the vacuum was established
prior to the run, except for the test described in Figure 23. The solar intensity,
water flow rate, and solar collector test specimen water inlet temperature were
monitored almost continuously during the tests and minor trim adjustments were
made as necessary.

## C. Data Acquisition System

The solar collector inlet and outlet thermocouples were used to deter-
mine the temperature rise across the collector. These two thermocouples
had been very closely and accurately calibrated together for the best possible
accuracy. The flowmeter output was recorded such that the water flow rate
through the solar collector could be determined. The flowmeter had also been
closely calibrated. The output of the flowmeter inlet thermocouple was also
recorded. This measurement was used to determine a water density correction
factor to be applied to the flowmeter reading. These data points were the only

9
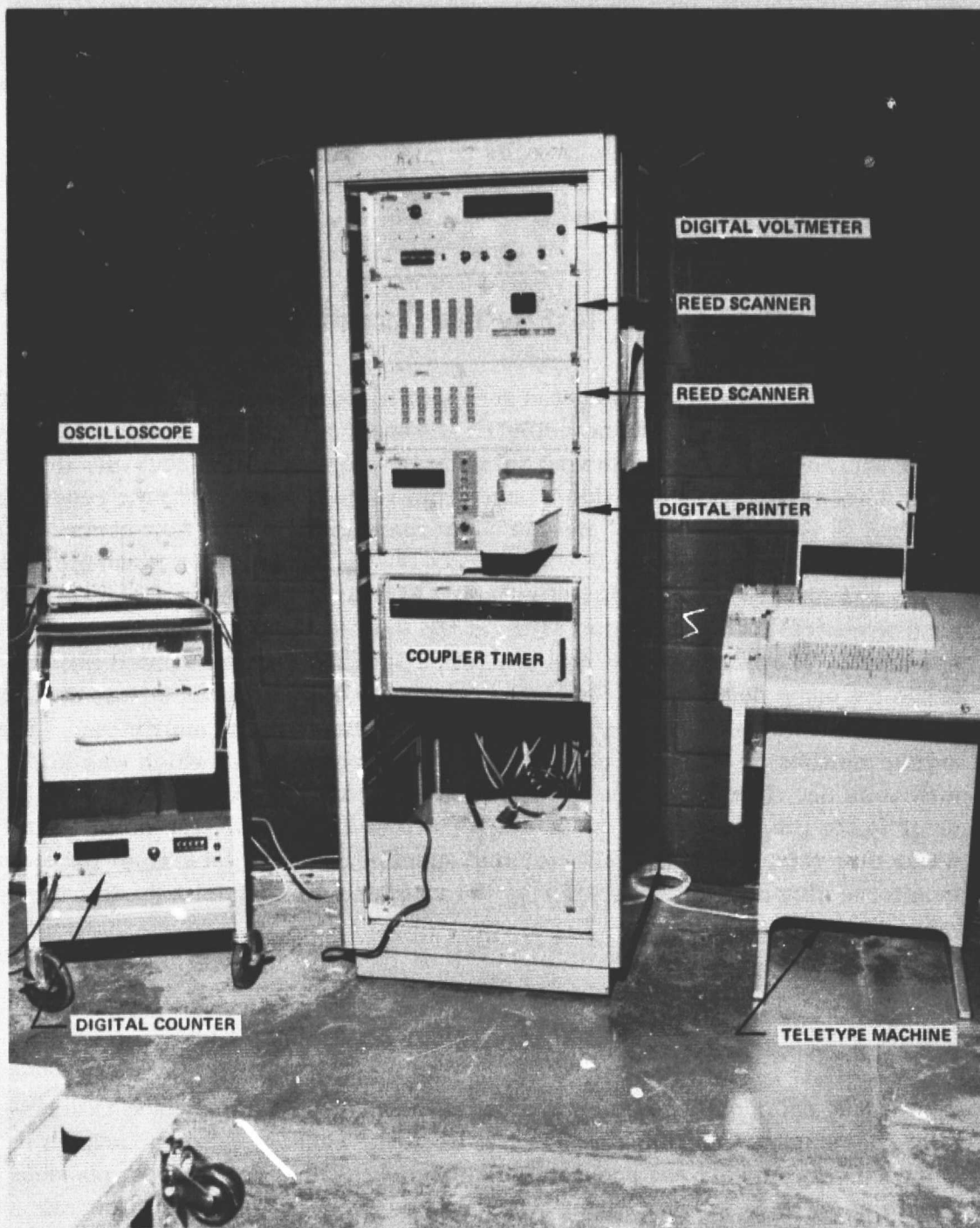
Figure 5. Data acquisition system.

ones used in determining the heat gain of those solar collector subsystems tested. The data acquisition system, however, sampled and recorded all the measurements shown on the schematic, Figure 1, every 10 min during each test. Prior to each test all adjustments were made, the system was given time to stabilize, usually approximately 20 min, and the data acquisition system (DAS) was set for a data "take" including the punched paper tape. During setup and stabilization the DAS was operating except for the punched paper tape portion of the teletype. The teletype typewriter portion was used to print data such that stabilization could be determined. Figure 5 is a photograph of the DAS.

DAS systems operation basically was as follows. The clock timer or coupler timer activated the reed scanner every 10 min causing it to scan each of the 18 measurements on the test system. The scanner acted to momentarily connect each of the 18 measurements to the input of the integrating digital voltmeter one at a time, in order, and to cycle back to "off" when completed. The integrating digital voltmeter, which had autoranging capability and the capability for measuring frequency and period, was also programmed to the correct mode by the reed scanner for each measurement to be made. The integrating digital voltmeter measured the signal from each channel and then caused the digital printer and the teletype to record the data. The digital printer was only used until the computer program was completed. From that point on the digital printer was turned "off" and the teletype was used exclusively. The DAS output originally was a paper strip with the time of day and the measurement of each channel from the digital printer. Data in this format had to be reduced, and calculations had to be done on a calculator. After the computer program was completed, the teletype was used and the DAS output was a typewritten sheet with the same data that the digital printer had provided, plus a punched paper tape compatible with the computer high speed tape photoreader (Fig. 6). When the data were reduced and calculated by hand, the data from typical tests required from 2 to 4 h to complete. After the computer program was completed, data reduction required approximately 15 min.

The DAS performed very well during these tests.


## D. Data Reduction System


The equipment utilized for data reduction on the majority of these tests is shown in Figure 6. Operation was as follows. With the computer, high speed photoreader, and teletype machine "on," a programming tape was fed

Figure 6. Data reduction system.

HP2116C COMPUTER

HIGH SPEED
PHOTOSCANNER

HIGH SPEED
TAPE PUNCH

TELETYPE MACHINE

into the high speed photoreader which loaded the program into the computer. (The computer routinely retains a certain basic program in its memory.) Once the program was loaded into the computer memory, a data tape could be fed into the high speed photoreader, after certain title and test conditions were entered, in response to computer requests for required variable information such as area of the collector, number of sets of data, etc.

The high speed photoreader and computer read the data tape one set of data at a time and performed certain operations on the raw data and stored the required information in its memory. These operations included converting thermocouple millivolt readings into temperatures, converting flowmeter pulses into water flow rates, adjusting mass flow with a density correction factor, and calculating the temperature rise across the collector. Once the computer stepped through all the sets of data, it completed the calculations and printed out heat gain, temperature rise across the collector, volumetric and mass flow rates, inlet temperature, temperature at the inlet of the flowmeter, and the mean and standard deviation (across the total number of sets of data) for each of the columns of data printed out. For dry stagnation tests, the computer was programmed to "look" at the three thermocouples attached to the solar collector plate itself, to pick the warmest one and convert the millivolt reading into temperature, and to print out that temperature versus time in two columns. The data reduction system performed very well and was a tremendous time saving device.

# E. Solar Simulation

Since the solar simulator was to be used as a substitute for sunlight, there was concern that the spectral energy of the xenon tube type unit would not closely match solar radiation and that this would seriously affect the heat gain results obtained from simulator tests. In an effort to determine the spectral differences between sunlight and the solar simulator to be used for these tests, a spectroradiometer was used to measure the radiation intensity of both at various wavelengths from 380 through 1050 nm. The results of these measurements are shown in Figure 7.

An analysis of Figure 7 reveals that the 6 kW xenon tube type solar simulator has a lower energy intensity in the longer wavelength ultraviolet and visible light range, 380 through 750 nm, than sunlight, but a considerably

13
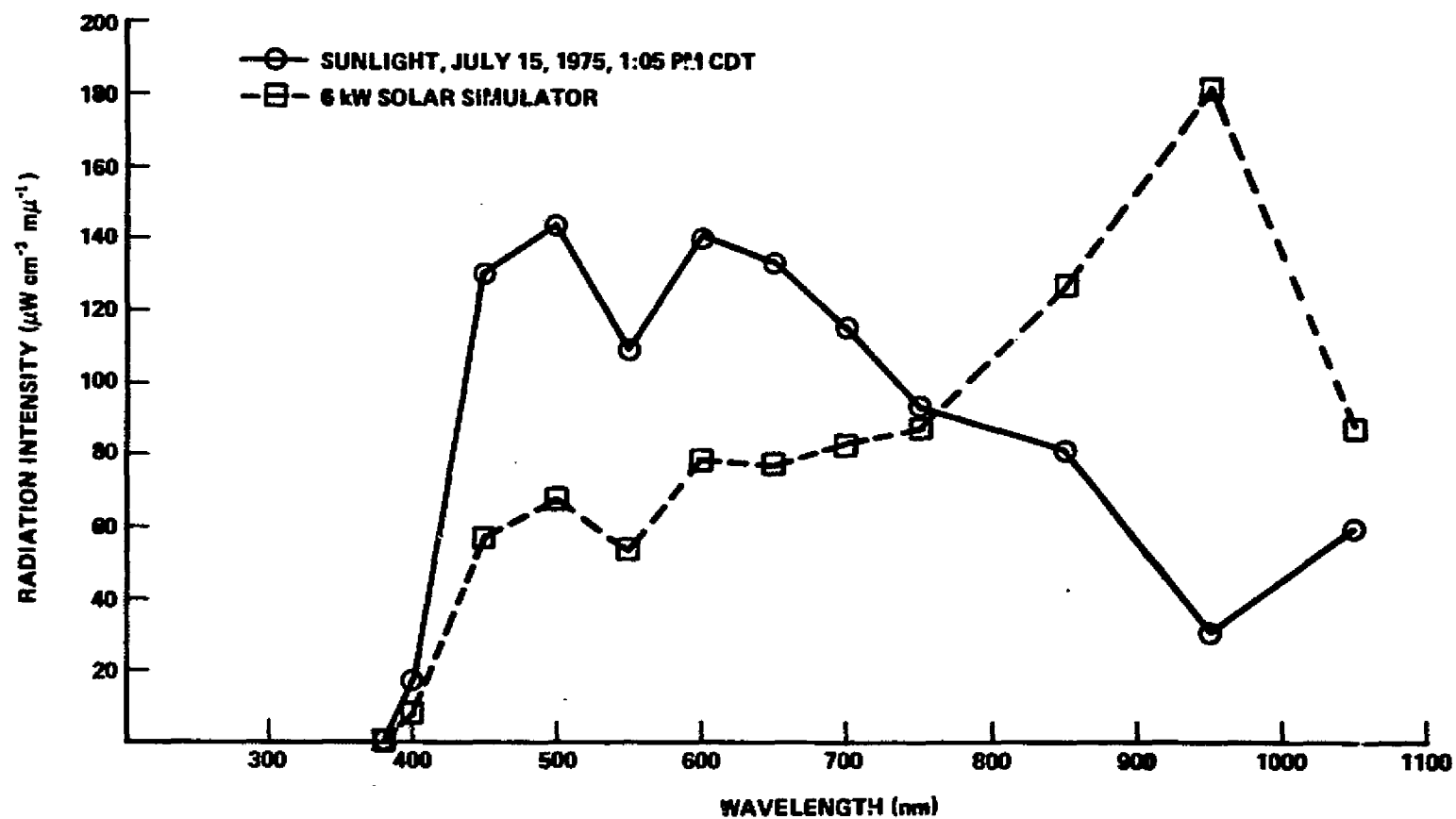
Figure 7. Comparison of spectral intensity of solar simulator and sunlight.

higher intensity in the infrared range, 750 through 1050 nm. The spectroradiometer used had been calibrated by the U. S. Army Metrology and Calibration Center, Redstone Arsenal, Alabama, DRSMI-MSM. A further verification of the general energy spectrum curve shapes of both types of radiation sources was made by a literature check. A typical energy spectrum curve for a 5 kW xenon lamp was found in a publication by Koller [1]. Figure 8 is a copy of that graph which was taken from a General Electric Co. bulletin. A curve of solar energy electromagnetic spectra was located in a publication by Krider and Kreith [2]. For a copy of this curve, see Figure 9. In general, the measured results shown in Figure 7 agree relatively well with published data. Even though the simulator energy spectrum did not match the solar energy spectrum over the entire wavelength spectrum very well, it was decided to continue the tests to compare simulator data with sunlight data, which was planned later in the test series.

The 6 kW xenon solar simulator utilized was powered by a dc source. The dc source was equipped with a variable current control feature that was used to adjust the intensity of the lamp. The smaller vacuum tube collector tests were run at approximately the 4550 W level of the solar simulator, but the insulated box collector required that the simulator be operated at approximately the 5600 W level because of the collector's larger size. The collector's larger size dictated that it be positioned further from the solar simulator in order for the beam to cover the collector's entire surface. Then, since the distance was greater, the beam intensity had to be raised to maintain approximately the same flux level at the collector surface.

## F. Solar Simulator Operation

With the solar simulator current control set such that a minimum stable beam could be maintained, a momentary switch was pressed to apply a high voltage ac signal across the xenon lamp terminals to start. With a stable operating lamp, the current control was slowly increased to the desired intensity level. Beam intensity was generally set utilizing the lamp voltage and current measurements provided on the control panel. Beam intensity was checked periodically with the pyrheliometer. During the initial setup of each type of collector, the test equipment and collector mounting board were repositioned and moved to center the collector in the lamp beam, to square up the collector with the beam, and to obtain a beam intensity close to the desired 0.75 solar
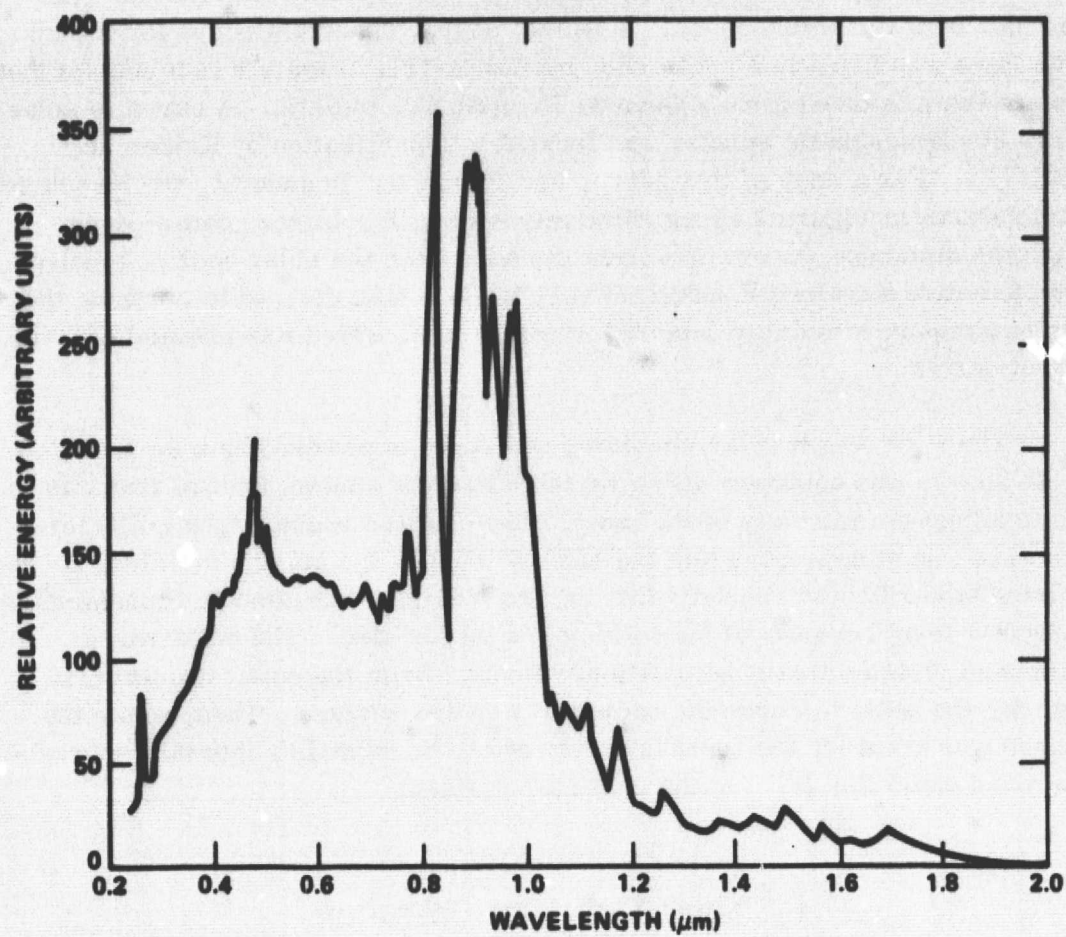
NOTE: ELECTRODE RADIATION EXCLUDED.

Figure 8. Spectral energy distribution of a typical
5 kW xenon lamp.

Figure 9. Electromagnetic spectra of solar radiation.
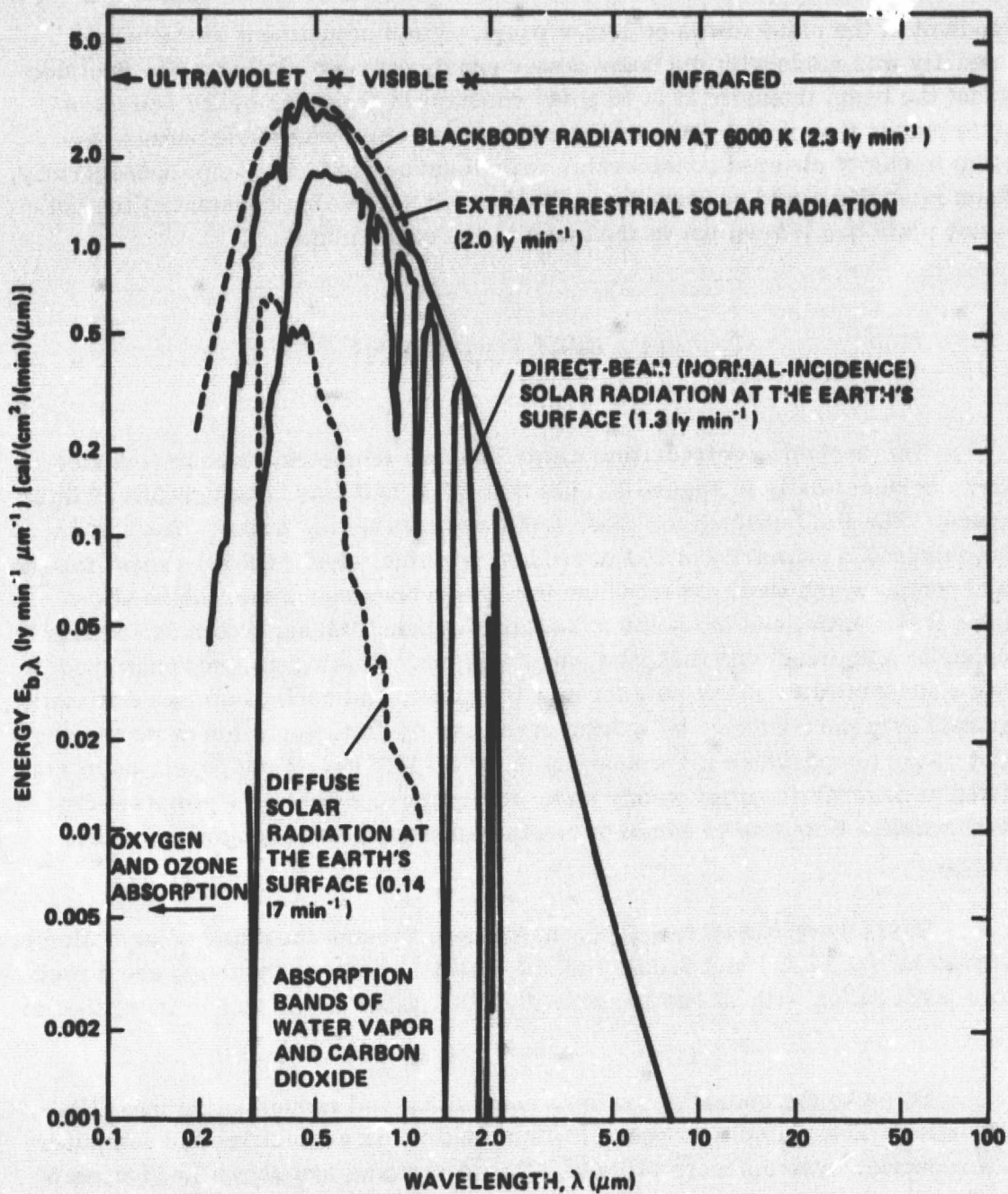
NOTE: THE BLACKBODY RADIATION AT 6000 K IS REDUCED BY THE SQUARE OF THE RATIO OF THE SUN'S RADIUS TO THE AVERAGE DISTANCE BETWEEN THE SUN AND THE EARTH TO GIVE THE FLUX THAT WOULD BE INCIDENT ON THE TOP OF THE ATMOSPHERE.

17

constant in the plane of the collector panel. Final adjustment of the beam intensity was made with the beam power supply current control. The decision to set the beam intensity at 0.75 solar constant in the plane of the collector plate rather than in the plane of the outer cover plate was made because the beam intensity changed considerably with distance from the lamp; consequently, beam intensity would not have been the desired 0.75 solar constant at the collector plate had it been set in the plane of the cover plate.

## III.  TEST EQUIPMENT

The portable recirculating water flow and temperature control device is shown schematically in Figure 1. Figures 2, 3, and 4 are photographs of this device. The fluid utilized for these tests was potable tap water. The system was fabricated primarily of 304 corrosion resistant steel (CRES) except for the fluid pump, which was cast iron; the flowmeter body and rotor, which were Ryton R-4 plastic; and the solar collector test panel tubing, which varied from copper to aluminum with different panel designs. Testing was accomplished with a constant water flow rate through the panel, and each panel was evaluated for heat gain performance by testing in the steady state condition at increasing inlet water temperature increments to 82.2°C (180°F). Most panels were also tested at several different steady state flow rates to establish a more nearly ideal specific flow rate at which to run the increasing inlet temperature test series.

Tests were run on two different sizes of vacuum insulated solar collectors, 0.01579 m$^2$ (0.17 ft$^2$) and 0.08129 m$^2$ (0.875 ft$^2$), and one insulated sheet metal box configuration with an outer common window glass cover and an inner Tedlar cover.

To make the operations of data acquisition and reduction the least time consuming and as simple as possible, automatic data acquisition and computer data reduction systems were utilized. These systems are shown in Figures 5 and 6, respectively. The coupler/timer was set such that one complete set of data was taken automatically every 10 min.

For a detailed list of the equipment used, see the appendix.

18

# IV. TEST PROCEDURE

Since the purpose of this test program was to evaluate various coatings
for possible use on solar collectors and to compare different solar collector
designs, a test method was devised such that the coatings and collectors could
be characterized. The same test procedure was utilized insofar as possible
for each candidate coating and for each solar collector design, such that the
data obtained could be compared. The only deviations from this policy were
necessary because of differences in solar collector size and because of minor
test equipment limitations. The test equipment limitations will be discussed in
detail later.

Tests of several different solar collector coatings, two different substrate
materials, and two different collector designs were made, as well as numerous
other individual parameter change experiments that were devised to establish
characteristic curve shapes, trends, and interdependencies.

The following is a list of the different coatings and substrate materials
tested, grouped by solar collector design in which they were tested:

1. Replaceable Panel Evacuated Tube Collector, Solar Simulator
Source

    a. Black nickel coating on copper substrate with copper tubing,
brazed assembly, $\alpha = 0.79$, $\epsilon = 0.05$

    b. Oxidized nickel sulfamate on aluminum substrate, aluminum
tubing, brazed assembly, $\alpha = 0.80$, $\epsilon = 0.05$

    c. Oxidized nickel sulfamate on copper substrate, copper tubing,
brazed assembly, $\alpha = 0.80$, $\epsilon = 0.05$

    d. 3M Nextel black velvet paint on aluminum substrate, aluminum
tubing, brazed assembly, $\alpha = 0.93$, $\epsilon = 0.91$

    e. Rustoleum flat black paint on aluminum substrate, aluminum
tubing, brazed assembly, $\alpha = 0.92$, $\epsilon = 0.87$.

Figure 10 is a photograph of four of the solar panels tested in the
replaceable panel vacuum tube collector. Figure 11 is a photograph of the
replaceable panel evacuated tube collector.
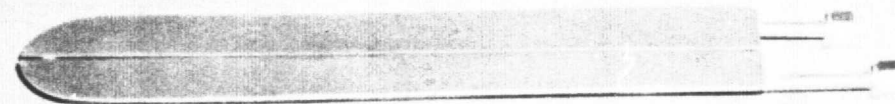
OXIDIZED Ni SULFAMATE COATING ON Al
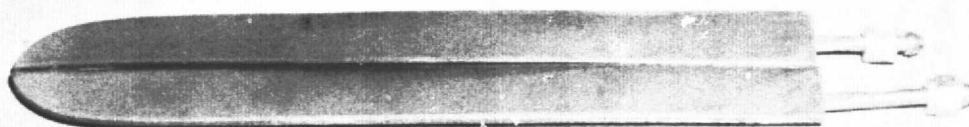
OXIDIZED Ni SULFAMATE COATING ON Cu
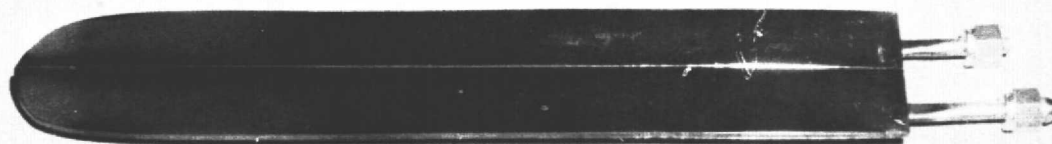
BLACK Ni COATING ON Cu
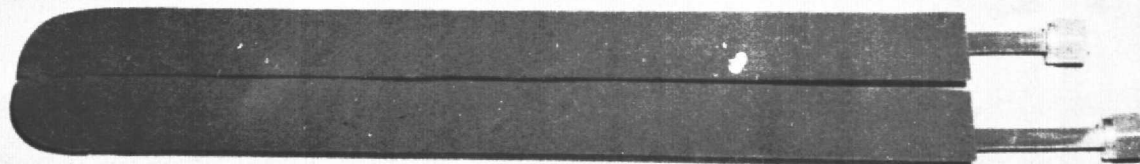
RUSTOLEUM FLAT BLACK PAINT ON Al

Figure 10.   0.01579 m$^2$ replaceable type solar collector panels for evacuated tube collector.
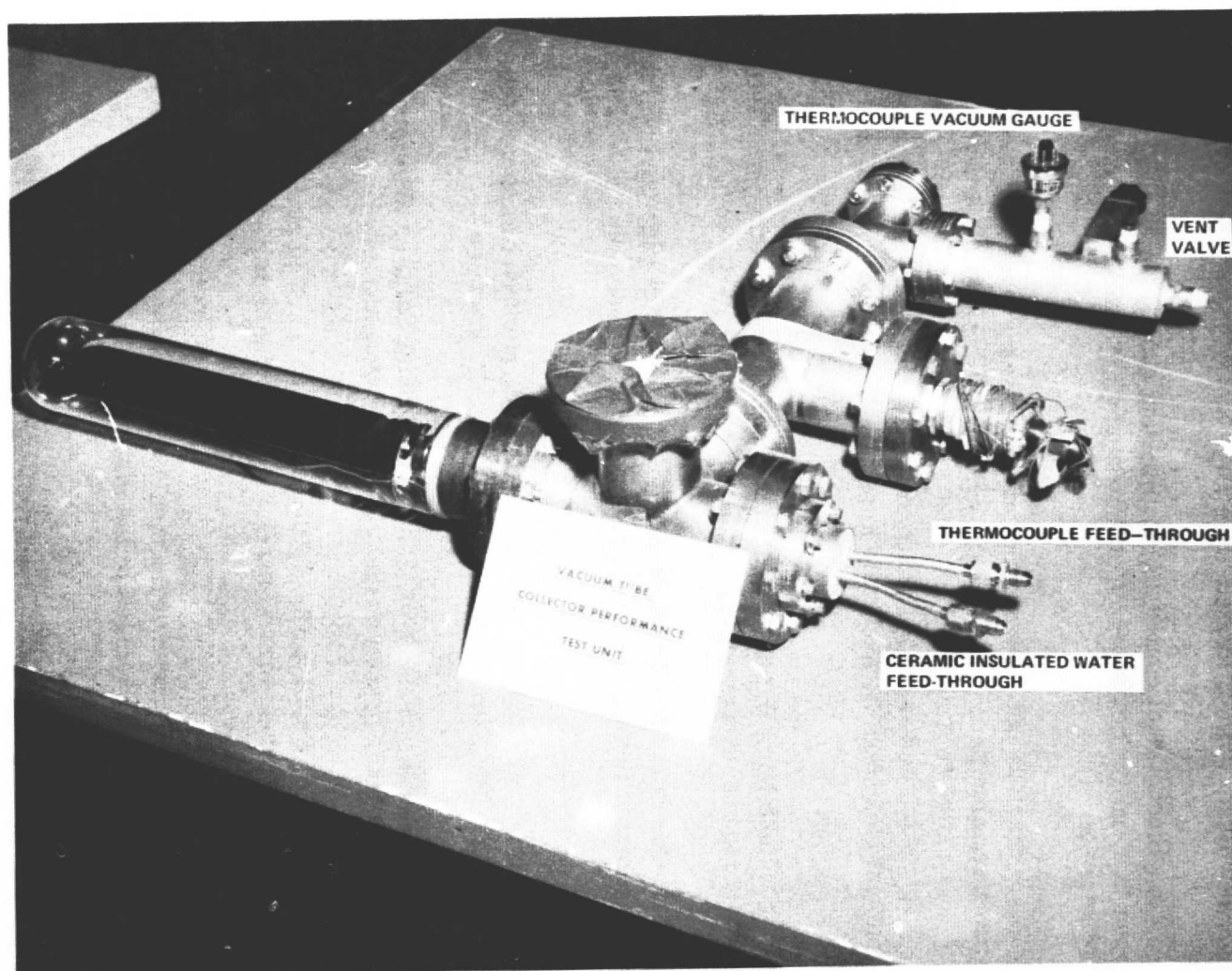
Figure 11.  Replaceable panel evacuated tube collector (0.01579 m² area).

2. Insulated Box Collector, Solar Simulator Source

a. One coat P60G2 primer filled with S-28 black pigment on aluminum substrate, aluminum tubing, brazed assembly, $\alpha = 0.93$, $\epsilon = 0.90$

b. Black nickel coated air conditioning condenser coil, 2.54 cm thick, open fins, no reflector behind coil, $\alpha$ and $\epsilon$ not available because of irregular surface

c. Black nickel coated air conditioning condenser coil, 2.54 cm thick, open fins, aluminum foil reflector behind coil, $\alpha$ and $\epsilon$ not available

d. Black nickel coated air conditioning condenser coil, 2.54 cm thick, fins bent closed on the back side to form a light trap, $\alpha$ and $\epsilon$ not available

e. Rustoleum flat black paint (aerosol spray) on aluminum substrate, aluminum tubing, brazed assembly, $\alpha = 0.92$, $\epsilon = 0.87$

f. One coat P60G2 primer filled with S-28 black pigment on aluminum substrate, aluminum tubing, thermal bonding material assembly, $\alpha = 0.94$, $\epsilon = 0.85$

g. One coat Caldwell No. C 1077-3 black paint on aluminum substrate, aluminum tubing, brazed assembly, $\alpha = 0.87$, $\epsilon = 0.64$

h. One coat Caldwell No. 129-386 flat black paint on aluminum substrate, aluminum tubing, brazed assembly, $\alpha = 0.92$, $\epsilon = 0.87$

i. One coat P60G2 primer filled with S-28 black pigment on aluminum substrate, aluminum tubing, brazed assembly, tube side toward solar simulator, $\alpha = 0.94$, $\epsilon = 0.85$.

Figure 12 is a photograph of the insulated box collector. Four representative samples of solar panels tested in the insulated box collector are shown in Figure 13.

3. Insulated Box Collector, Actual Sunlight Source — One coat P60G2 primer filled with S-28 black pigment on aluminum substrate, aluminum tubing, brazed assembly, tube side toward Sun, $\alpha = 0.94$, $\epsilon = 0.85$.
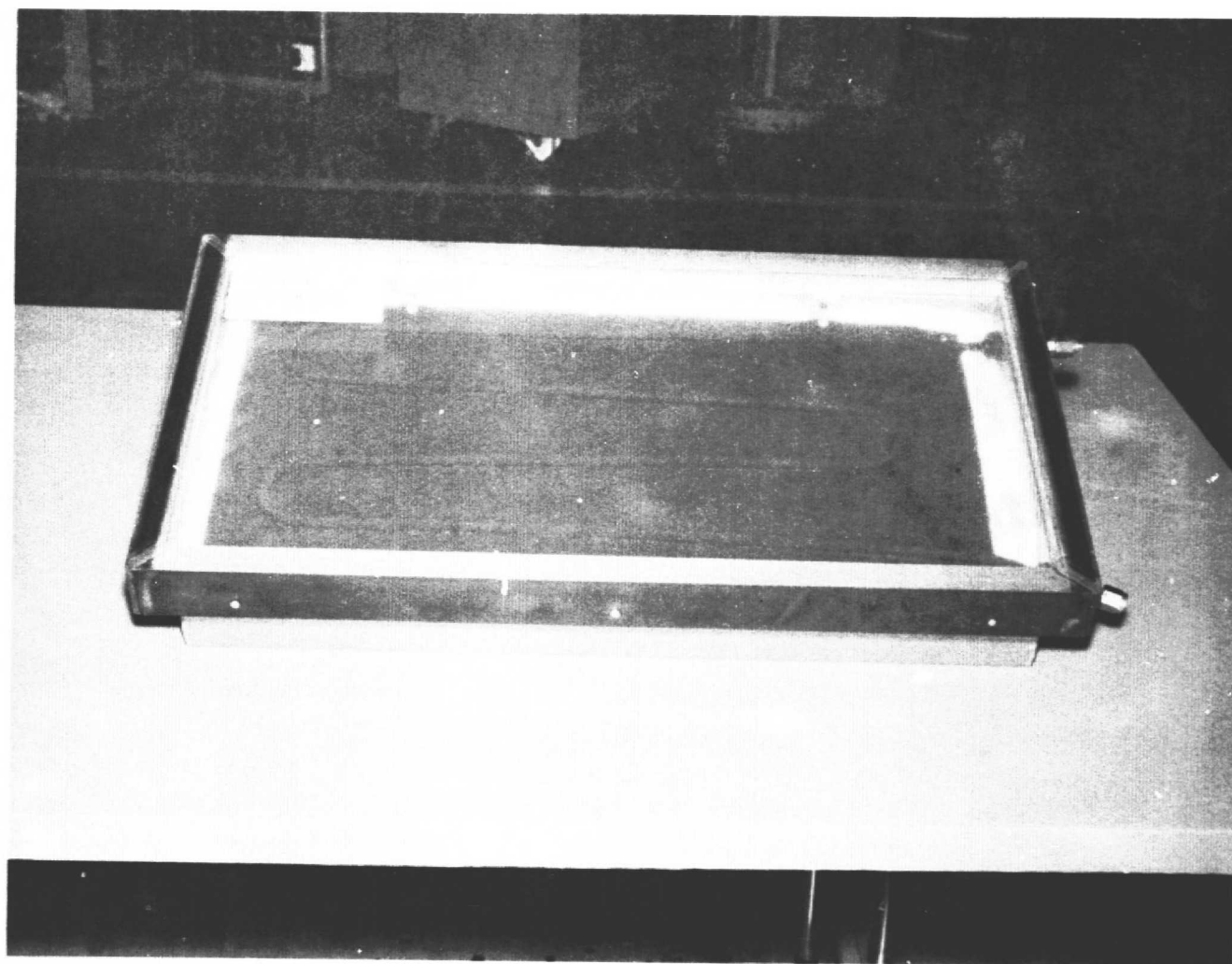
Figure 12.   Replaceable panel insulated box collector ($0.1858$ m² area).

R. GUMBS POLYVINYL BUTYRAL PAINT
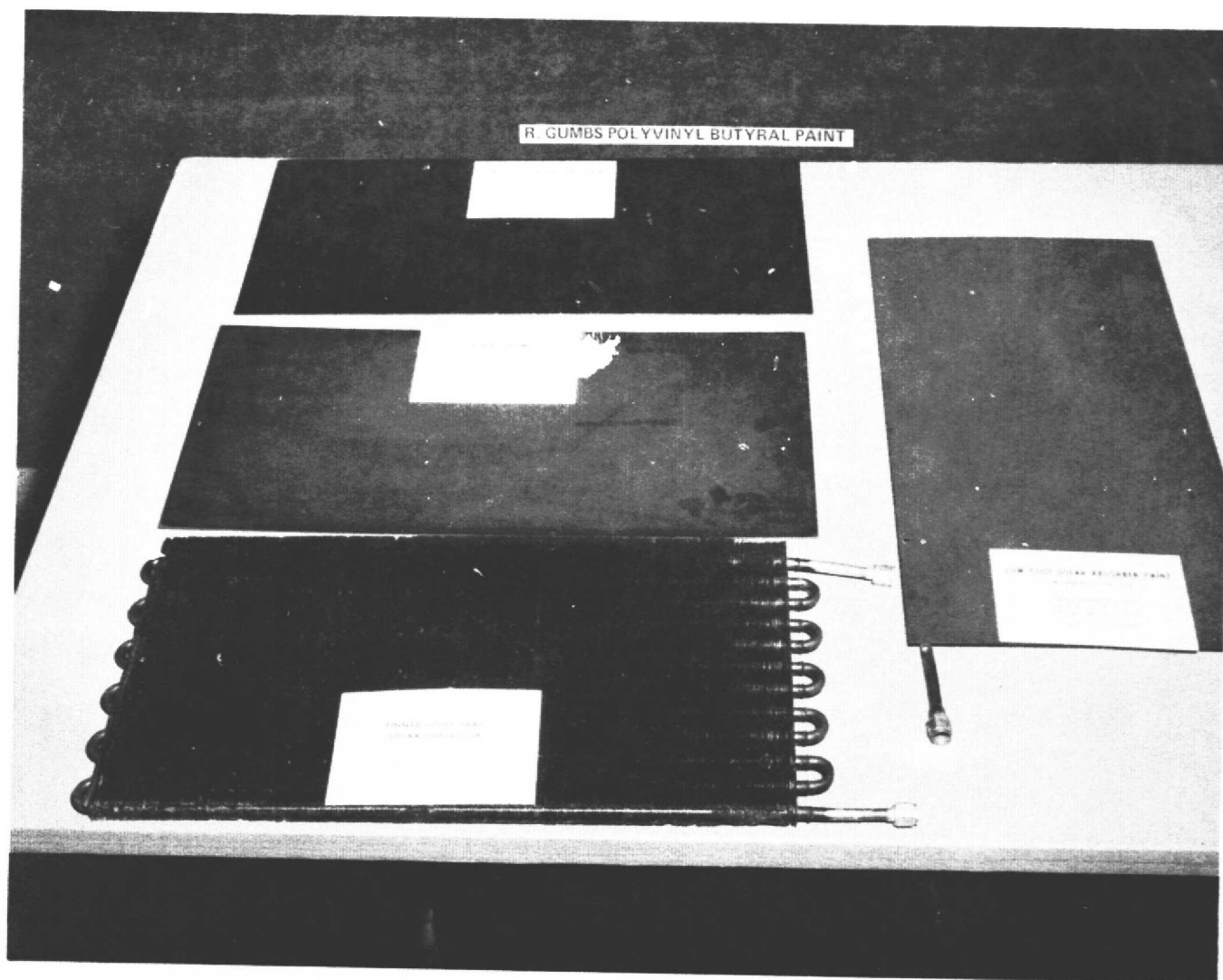
Figure 13. Solar panels for replaceable panel insulated box collector.

4. Sealed Glass Tube Evacuated Collector, Actual Sunlight Source —
Black nickel coated copper substrate, copper tubing, brazed assembly, evac-
uated Pyrex glass envelope, $\alpha = 0.87$, $\epsilon = 0.05$.

The solar collector coatings listed above were manufactured as follows:

1. Black Nickel Coatings — This finished coating was achieved by bright
nickel electroplating the surface and black nickel plating it to a precise thickness.
The precise thickness was necessary to create the desired optical properties.

2. Oxidized Nickel Sulfamate Coatings — This finished coating was
achieved by nickel sulfamate electroplating the surface and oxidizing this coating
in air at $510°C$ ($950°F$) for approximately 8 min to create the desired optical
properties.

3. Painted Coatings — The painted surfaces were achieved by spraying.
Efforts were made to apply the paint uniformly to a thickness of approximately
0.0076 mm (0.0003 in.) to optimize the optical properties. The painted sur-
faces were oven cured (dried) at approximately $177°C$ ($350°F$) for 2 h.

A list of different tests conducted on the solar panels, substrate mate-
rials, and solar collector designs described previously follows:

1. Solar collector dry stagnation temperature versus time

2. Effect of vacuum insulation on dry stagnation temperature

3. Effect of flow rate on heat gain

4. Effect of inlet temperature on heat gain versus flow rate performance

5. Effect of inlet temperature on heat gain

6. Effect of vacuum insulation on heat gain versus inlet temperature
performance

7. Effect of reflectors on vacuum tube collector heat gain versus inlet
temperature performance

8. Effect of thermal bonding material versus brazing/welding the
tube-to-plate interface on heat gain versus inlet temperature

9. Effect of backside radiation on vacuum tube collectors.

This list of tests included those which were considered "special" and/or "one time" as well as those which were considered a part of the "standard" test series to be conducted on all solar collectors to be tested with the solar simulator. It should be noted that not all of the "standard" tests were planned during the actual sunlight tests because of the time which would have been required. The "standard" test series for solar collectors to be tested with the solar simulator follows.

---

### Standard Test Sequence

Dry Stagnation Test

Heat Gain Versus Flow Rate

| $0.01579 \text{ m}^2$ | $(0.17 \text{ ft}^2)$ Panel | $0.1858 \text{ m}^2$ | $(2 \text{ ft}^2)$ Panel |
|---|---|---|---|
| 0.76 liter/h | (0.2 gal/h) | 1.14 liters/h | (0.3 gal/h) |
| 1.14 liters/h | (0.3 gal/h) | 2.27 liters/h | (0.6 gal/h) |
| 1.70 liters/h | (0.45 gal/h) | 3.41 liters/h | (0.9 gal/h) |
| 2.27 liters/h | (0.6 gal/h) | 4.54 liters/h | (1.2 gal/h) |
| | | 5.68 liters/h | (1.5 gal/h) |
| | | 6.81 liters/h | (1.8 gal/h) |
| | | 7.95 liters/h | (2.1 gal/h) |

Heat Gain Versus Inlet Temperature (All Panel Sizes)

| 26.7°C | (80°F) Inlet Temperature |
|---|---|
| 48.9°C | (120°F) Inlet Temperature |
| 71.1°C | (160°F) Inlet Temperature |
| 82.2°C | (180°F) Inlet Temperature |

Dry Stagnation Test (Degradation or Optical Properties Change)

---

Tests of the different coatings and solar collectors with both the solar simulator and in actual sunlight were performed in the order shown primarily due to the availability of hardware for test.

# A. Replaceable Panel Evacuated Tube Collector

This configuration consisted of a cylindrical Pyrex glass envelope attached to a metal (con-flat) flange through a Kovar glass-to-metal seal. The metal flange provided the capability to change the solar collector panel as desired. A cross sectional view of this collector is shown in Figure 14. The glass envelope and metal flange were connected to additional vacuum connections to provide sufficient ports and feed-throughs for instrumentation, water flow tubing, the vacuum system and its measuring devices, and a vent valve. A pictorial view of this equipment is shown in Figure 11. The solar collector panels tested were 30.48 cm (1 ft) in length with an area of 157.9 cm$^2$ (0.17 ft$^2$). Five solar panels of this configuration were tested including four different coatings and two different substrate materials. A pictorial view of four of these collectors is shown in Figure 10.

The test apparatus was set up as shown schematically in Figure 1 and pictorially in Figures 2, 3, and 4 with associated instrumentation as previously described. It was decided that a solar simulator integrated flux level of 0.75 solar constant, or approximately $3.654 \times 10^6$ J/m$^2$/h (1014.73 W/m$^2$/h or 321.75 Btu/ft$^2$/h), would be utilized since this value approximates the highest incident energy level normally experienced in this geographical region.

The vacuum system was used to maintain a pressure of less than $1.333 \times 10^{-2}$ N/m$^2$ ($1 \times 10^{-4}$ mm Hg) during all tests in which a vacuum was desired. A liquid nitrogen cold trap was used to ensure that no pump oil vapor could contaminate the collector surface.

The water flow and temperature control device was not operated during the first and last tests of a particular panel, since the intent of those tests was to determine the maximum temperature attainable with no water in the collector. This condition has been called the dry stagnation temperature of a collector. The second dry stagnation test was conducted to evaluate coatings to determine short term changes in optical properties. All other tests performed on each panel were made with a constant flow rate. These water flow tests were made in two different series. The first series of tests was made to study the performance, heat gain versus water flow rate, or specific flow rate of each panel tested such that an optimum flow rate could be chosen for the later tests. The first series of tests was made with inlet water temperatures generally between 26.67°C (80°F) and 37.78°C (100°F).

SOLAR PANEL

GLASS ENVELOPE

WATER FLOW TUBE

METAL FLANGE
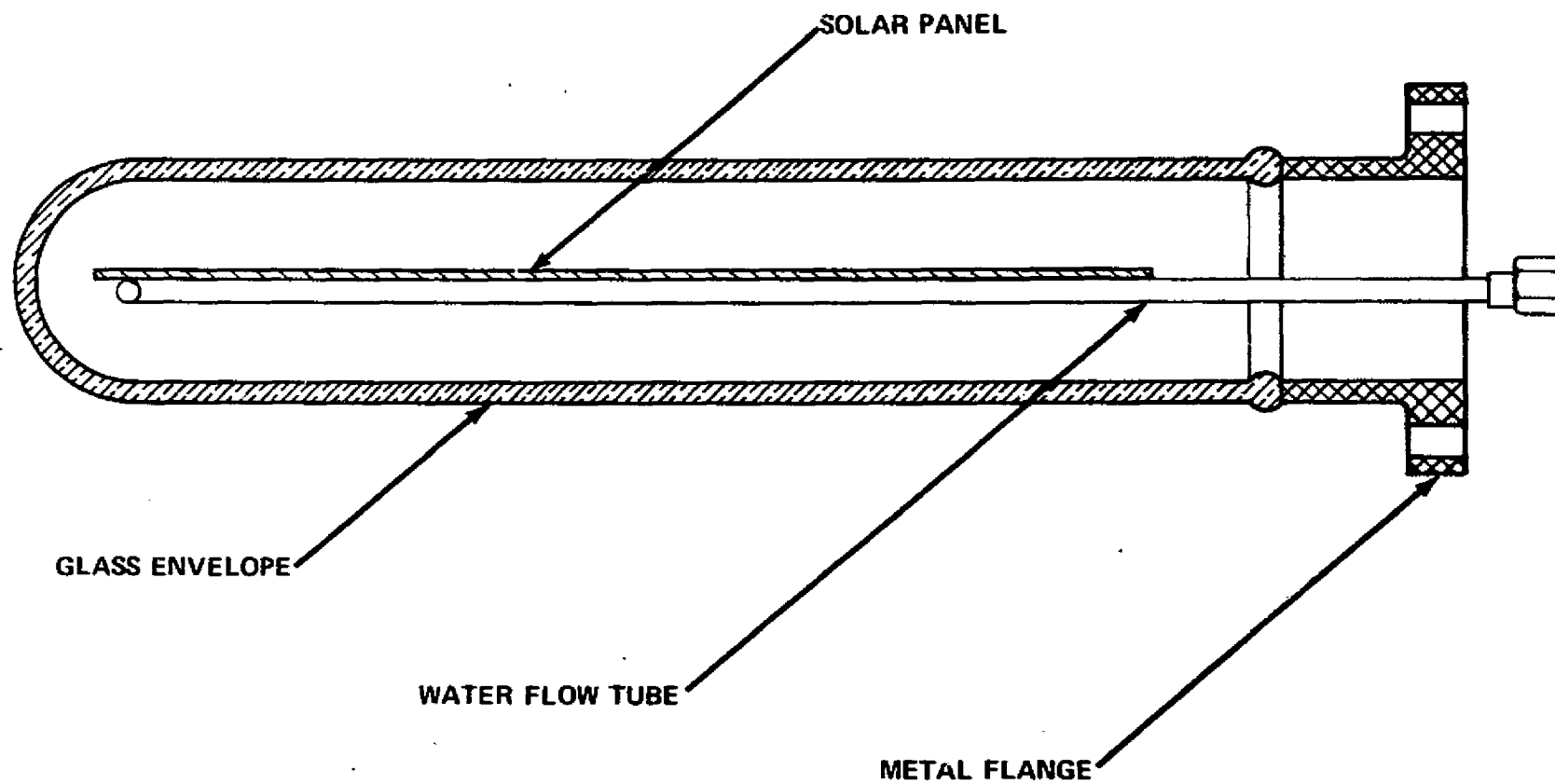
Figure 14.   Replaceable panel type vacuum tube solar collector.

The second series of tests was made to evaluate performance and heat gain versus inlet water temperature with inlet temperatures ranging from 26.67° to 82.22°C (80° to 180°F). Each test was run at a steady state flow, inlet temperature, and solar simulator intensity for a sufficient length of time to assure stability and to obtain several 10 min data point slice times so that data averaging could be employed.

## B.  Insulated Box Collector

This configuration consisted of an insulated sheet metal box with an outer cover of common window glass and an inner cover of Tedlar plastic film. The solar panel was replaceable. Nine different panel configurations were tested. The panel size was 0.1858 m$^2$ (2 ft$^2$). Figure 15 is a cross sectional view of this configuration.

The test apparatus was set up as described previously except that the vacuum system was not used. (This solar collector design was not evacuated.) The solar simulator was utilized for these tests. The tests made on these panels were the same as those described previously except that the water flow rates were higher because of the larger panel area. Dry stagnation tests were performed as a first and last test on each panel. Between these two tests were the two test series; the first was an incremental flow rate versus heat gain series, and the second was an incremental inlet water temperature versus heat gain series. Each incremental test was run at a steady state flow, inlet temperature, and solar simulator intensity long enough to assure stability and to obtain several data point slice times such that data averaging could be employed.

## C.  Insulated Box Collector in Sunlight

The configuration for these tests was the same as previously given in Section IV. B except that the solar simulator was not used.

This test sequence was limited to a dry stagnation run plus an incremental inlet water temperature versus heat gain series. The solar collector was stationary but was positioned normal to the insolation at solar noon. The pyrheliometer was also stationary and in the plane of the solar collector, approximately 0.75 m from the center of the collector. A continuous strip chart recording of

COLLECTOR PANEL

GLASS

TEDLAR

WOOD SPACER

FLOW TUBE

INSULATION

PHENOLIC INSULATOR STANDOFF
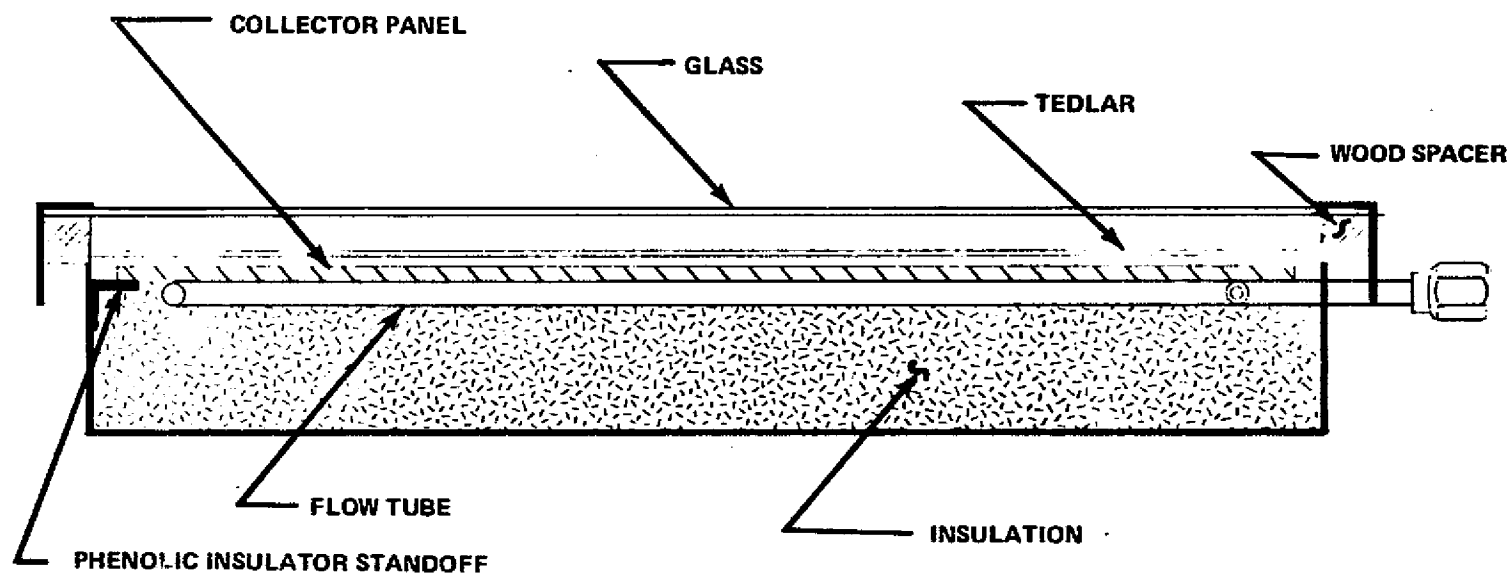
Figure 15.   Replaceable panel insulated box solar collector.

pyrheliometer output was made during all outdoor tests. Data were taken and reduced across the entire day; however, only the data taken at or within 1.5 h of solar noon were used for the heat gain versus inlet temperature curves. Days and times of high insolation were used such that normalization of the data to 0.75 solar constant would introduce a minimum of error. Data utilized were taken during times when solar insolation varied from approximately 0.50 to 0.71 solar constant.

## D. Sealed Tube Evacuated Collector in Sunlight

This configuration consisted of an evacuated and sealed Pyrex glass envelope containing a black nickel coated copper panel. The panel was 0.91 m (3.0 ft) in length with an area of 0.081 $m^2$ (0.875 $ft^2$). The water flow tubing was copper and was brazed to the panel. The glass envelope containing the panel was evacuated with an ion pumping system for 2 weeks with eight periodic heating cycles employed to bake out the glass envelope and black nickel plated panel prior to the time the 9.53 mm evacuation port was sealed permanently. Pressure inside the glass envelope when the seal was made was less than $6.67 \times 10^{-3}$ N/$m^2$ ($5.0 \times 10^{-5}$ mm Hg). The ion pumping system was utilized in evacuating the glass envelope to prevent contaminating the absorber surface or the glass envelope interior. The tubing-to-glass envelope feed-throughs were of the Kovar type. Figure 16 presents a pictorial view of this collector.

The tests performed on this collector included a dry stagnation run and two incremental inlet water temperature versus heat gain test series. One of these test series was performed at a specific flow rate equivalent to that run on the 0.01579 $m^2$ evacuated tube collector, and the other was at a specific flow rate equivalent to that used in tests on the 0.1858 $m^2$ insulated box collector. These two flow rate test series were intended to permit performance comparisons between the two different sizes of vacuum tube type collectors and between the vacuum tube and insulated box type collectors. A continuous strip chart recording of pyrheliometer output was made during all outdoor tests. Data were handled as described in Section IV.C.
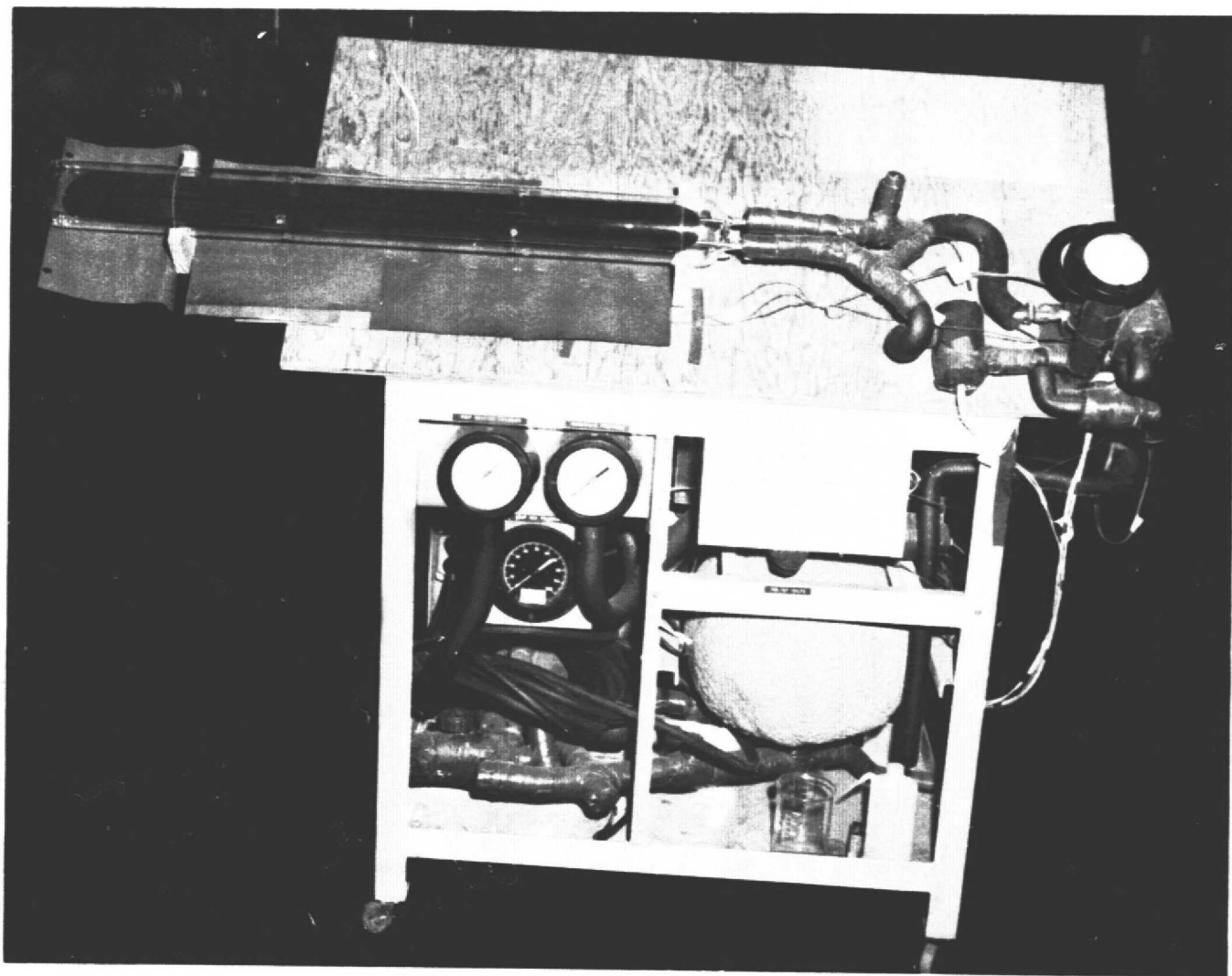
Figure 16. Solar collector test setup with sealed tube evacuated collector mounted in place.

# V. DISCUSSION AND RESULTS

## A. Replaceable Panel Evacuated Tube Collector

1. <u>Dry Stagnation Tests</u>. The purpose of these tests was to assist in characterizing the solar collector design and individual coating and substrate materials. Although the dry stagnation temperature achieved by a collector only gives an indication of its capability to produce usable heat energy, it does establish, for a particular ambient temperature and solar insolation value, that temperature at which the collector reaches equilibrium. For a particular ambient temperature and insolation value, the stagnation temperature of a collector is that temperature at or above which the collector can no longer perform a useful function.

Results of these tests are shown in Table 1 and Figure 17. It should be noted that the slope of the temperature rise curve was considerably influenced by the thermal mass of the collector plate and tubing; the two slow rise curves represent copper plates and tubing, whereas the others represent aluminum plates and tubing. Further, the thermal mass of the nickel sulfamate coated plate was slightly greater than that of the black nickel coated plate. The temperature-indicating thermocouples were in contact with the edge of the plates themselves. Each collector plate was fabricated in two halves with a small space between. The collector plate halves were brazed or welded to the tubing and were supported by the tubing. The thermocouples were imbedded in small pieces of Teflon which were machined such that they fit between the two collector plate halves. The thermocouple at the tubing turnaround bend invariably indicated the highest temperature. These highest temperatures were plotted in Figure 17. The stagnation temperatures that were eventually reached were the result of an equilibrium between heat input and heat losses. The input was the solar simulator energy absorbed by the collector plate, and the losses were that heat conducted away by the tubing and lost to the environment outside the evacuated tube and the collector plate's losses because of radiation from the warm collector plate surfaces to the glass enclosure.

An evaluation of Figure 17 reveals that with this solar collector design, emissivity is a very important factor in the stagnation temperature reached by a particular coating or coating/substrate combination. As can be observed, the nonselective coatings (the paints) had considerably higher absorptivities than the selective coatings; however, they did not approach the maximum temperatures reached by the selective coatings.

### TABLE 1. STAGNATION TEST RESULTS — REPLACEABLE PANEL EVACUATED TUBE SOLAR COLLECTOR

| Coating and Substrate | Stagnation Temperature, | |
|---|---|---|
| | °C | (°F) |
| Nickel Sulfamate (Oxide) on Aluminum | 161.1 | (322) |
| Black Nickel Coating on Copper | 194.4 | (382) |
| Black Velvet Paint on Aluminum | 106.7 | (224) |
| Nickel Sulfamate (Oxide) on Copper | 188.9 | (372) |
| Flat Black (Rustoleum) Paint on Aluminum | 115.0 | (239) |

Test Conditions

6 kW Solar Simulator

0.75 Solar Constant (Integrated Flux Level)

$1.33 \times 10^{-2}$ N/m$^2$ ($1.0 \times 10^{-4}$ torr) Pressure

Zero Flow Rate (Dry Water Passages)

Ambient Temperature of 25°C (77°F)

2. Heat Gain as a Function of Flow Rate. The purpose of these tests was to establish a characteristic curve for each coating and substrate such that a flow rate could be selected for the subsequent tests, i.e., heat gain as a function of inlet temperature, that would not penalize the performance of a coating/substrate combination. The selection of a lower than nominal flow rate can affect heat gain and efficiency.

Results from these tests are shown in Figure 18. Data indicated that flow rates below a certain quantity, approximately 40.75 liters/m$^2$/h (1.0 gal/h/ft$^2$ or 0.17 gal/h/0.17 ft$^2$), caused a considerable decrease in collector heat gain and efficiency. The reason for this was that water temperature differential from inlet to outlet went up as the flow rate went down, causing a
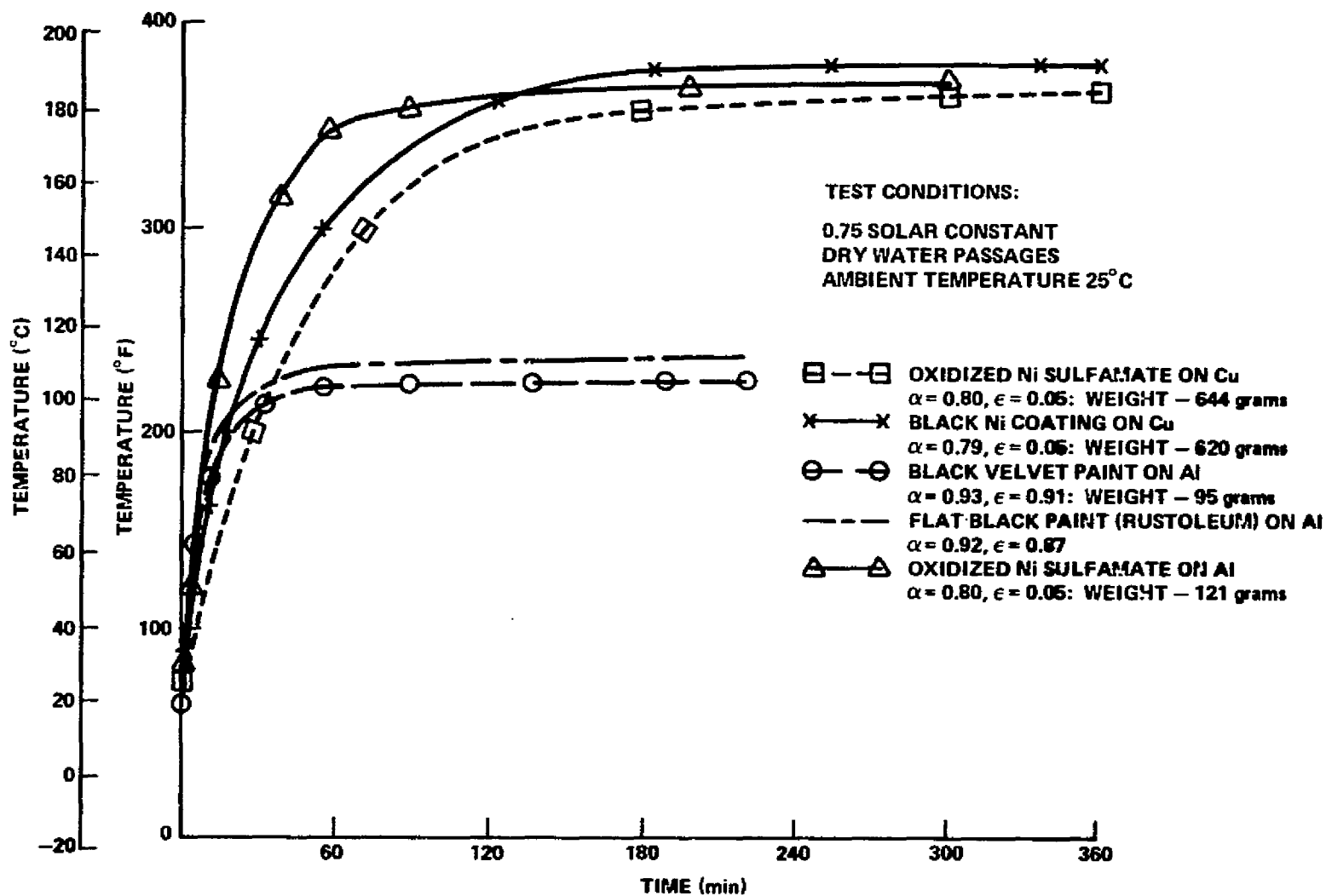
Figure 17.   Stagnation temperature comparison ($0.01579 \text{ m}^2$ replaceable panel evacuated tube collectors).

TEST CONDITIONS:

0.75 SOLAR CONSTANT
APPROXIMATELY 29.5°C INLET
TEMPERATURE
1.33 X 10⁻² N/m² PRESSURE
AMBIENT TEMPERATURE 25°C

O  OXIDIZED Ni SULFAMATE COATING ON Al
   $\alpha = 0.80$, $\epsilon = 0.05$
△  BLACK Ni COATING ON Cu
   $\alpha = 0.79$, $\epsilon = 0.05$
X  BLACK VELVET (FLAT BLACK PAINT) COATING
   $\alpha = 0.93$, $\epsilon = 0.91$
◇  RUSTOLEUM FLAT BLACK PAINT ON Al
   $\alpha = 0.92$, $\epsilon = 0.87$
□  OXIDIZED NICKEL SULFAMATE ON Cu
   $\alpha = 0.80$, $\epsilon = 0.06$

EQUIVALENT MSFC SOLAR HOUSE FLOWRATE 0.92 liters/h

HEAT GAIN (J/m²/h X 10⁶)

HEAT GAIN (Btu/h/ft²)

EFFICIENCY

4.0   100%   300
3.0   75%    200
2.0   50%
1.0   25%   100
0     0

FLOWRATE (gal/h)
0.1   0.2   0.3   0.4   0.5   0.6

FLOWRATE (liters/h)
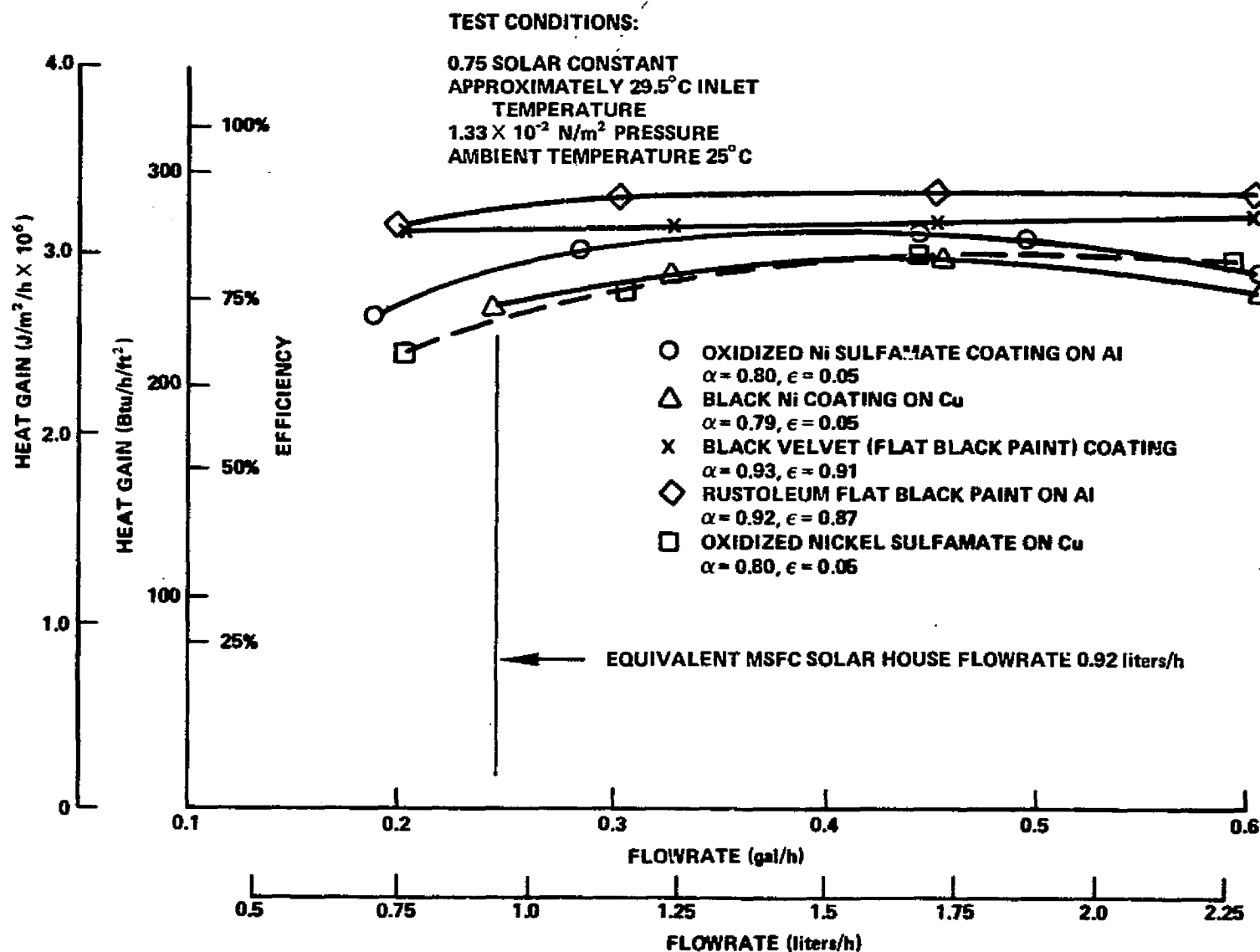0.5   0.75   1.0   1.25   1.5   1.75   2.0   2.25

Figure 18.  Typical heat gain versus flow rate curves (0.01579 m² replaceable
panel evacuated tube collectors).

higher average plate temperature which resulted in higher heat losses from the collector. It should be noted that these data were taken with relatively low water inlet temperatures.

Flow rate increases two to three times that mentioned, 40.75 liters/$m^2$/h (1.0 gal/h/$ft^2$), will increase performance at low water inlet temperatures; however, as will be shown later, at the higher inlet water temperatures that would be encountered in an operating system, the temperature differential across the collector would become small and the system's efficiency would suffer because of higher pumping costs, larger piping sizes, and higher heat losses.

A study of Figure 18 shows that the heat gain performance of the Rustoleum flat black paint was higher than the other coating/substrate combinations. As a result of this, the area of the Rustoleum painted panel was rechecked. As can be seen in Figure 10 the Rustoleum panel was radiused differently than the other panels on the end opposite the water connections. This caused the area of the Rustoleum printed panel to be approximately 4 percent larger than the other panels. It can also be noted that the paint extends out on the tubing almost to the water connection fittings, which further increased the panel's effective area. In summary, it is believed that the increased collector area, estimated to be approximately 6 percent, caused the high heat gain performance.

3. Heat Gain as a Function of Inlet Temperature. The purpose of testing each candidate coating in this fashion was to obtain quantitative data on the ability of this collector design and each coating and coating/substrate combination to convert solar type radiation into usable heat energy over a range of inlet temperatures that would be expected in an operating system. In an operating hot water system the reservoir temperature would slowly rise with several days of bright sunshine and moderate temperatures. The data presented in Table 2 and Figure 19 give an indication of the heat energy that could be collected per unit area at the collector with collector water inlet temperatures as shown, a solar intensity of 0.75 solar constant, a solar beam incidence angle with the collector of 90 degrees, and an ambient temperature of 25°C. A solar intensity of 0.75 solar constant, a beam energy normal to the collector surface, and an ambient temperature of 25°C were chosen such that collected heat energy data would reflect the highest values that could normally be expected in northern Alabama. For solar intensities less than those used for these tests, solar beam energy incidence angles less than 90 degrees, or ambient temperatures other than 25°C (77°F), calculations would be needed to determine the expected output.

37

## TABLE 2. HEAT GAIN VERSUS INLET TEMPERATURE TEST RESULTS — REPLACEABLE PANEL EVACUATED TUBE SOLAR COLLECTOR

| Coating and Substrate | Heat Gain, $J/m^2/h \times 10^6$ (Btu/$ft^2$/h) | | | | | | | |
|---|---|---|---|---|---|---|---|---|
| | 29.4°C | (85°F) | 48.9°C | (120°F) | 71.1°C | (160°F) | 82.2°C | (180°F) |
| Nickel Sulfamate (Al) | 3.06 | (269.4) | 2.06 | (181.6) | 1.02 | (89.9) | 0.596 | (52.5) |
| Black Nickel (Cu) | 2.87 | (252.6) | 2.08 | (183.4) | 1.32 | (116.1) | 0.921 | (81.1) |
| Black Velvet (Al) | 3.10 | (272.8) | 2.02 | (177.6) | 0.880 | (77.5) | 0.151 | (13.3) |
| Nickel Sulfamate (Cu) | 2.54 | (223.5) | 1.82 | (160.6) | 1.19 | (104.7) | 0.798 | (70.3) |
| Flat Black Paint (Al) | 3.34 | (293.7) | 2.27 | (200.2) | 1.07 | (93.9) | 0.529 | (46.6) |

Test Conditions

6 kW Solar Simulator, 0.75 Solar Constant

$1.33 \times 10^{-2}$ N/$m^2$ ($1.0 \times 10^{-4}$ torr) Pressure

1.14 liters/h (0.3 gal/h) Flow Rate, 71.9 liters/$m^2$/h (1.76 gal/$ft^2$/h)
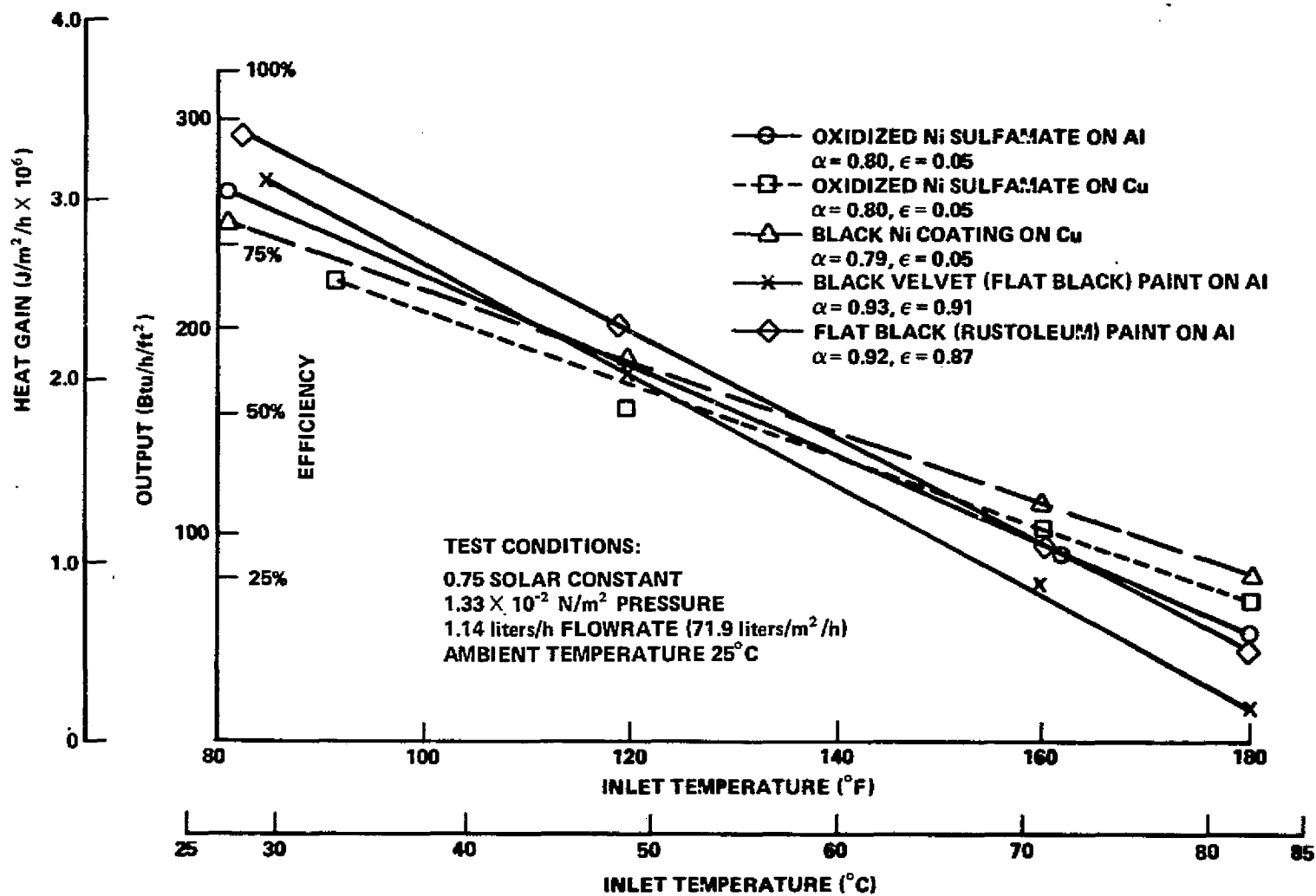
Ambient Temperature of 25°C (77°F)

Figure 19. Heat gain versus inlet temperature curves $(0.01579 \ m^2$ replaceable panel evacuated tube collector).

An analysis of the data shown in Figure 19 indicates that at the lower water inlet temperatures, the solar collector coating absorptivity was the controlling factor in the heat gain performance in this type of collector system design. At the high water inlet temperatures, the data indicated that the solar collector coating emissivity became the controlling factor in its heat gain performance. This was based on the fact that coatings with the lowest emissivity performed best at the high inlet temperatures. Again it can be noted that the performance of the Rustoleum painted panel was higher than the others because of the larger area.

The slopes of the curves shown are relatively steep indicating considerable heat loss with increasing inlet water temperature. The two black paints, as a nonselective coating class, had total heat gains of less than 16 percent at the high inlet temperatures in comparison to the low inlet water temperature conditions. Even the selective coatings, for instance the black nickel which was the better performer at high inlet temperatures, had heat gains of less than 33 percent at the high inlet temperatures in comparison to the low inlet water temperature conditions. The high apparent heat losses, even on panels with selective coatings, caused concern that conductive heat losses through the tubing might have been an appreciable percentage of the total heat gain involved, since the solar panels being evaluated were relatively small in area. The data presented were obtained after every effort was made to reduce line lengths from inlet and outlet thermocouples to the test panel and to insulate water lines, etc.

These results indicated that tests of larger scale panels were necessary to determine whether a "scaling factor" was involved. With larger solar panel sizes similar heat losses, in magnitude, would affect the data less since the total heat gain involved would be much larger. As will be discussed later, a larger vacuum insulated collector was tested and the performance was much better at the high inlet temperatures.

4. Effect of Vacuum Insulation on the Heat Gain as a Function of Inlet Temperature Performance. The purpose of this test was to determine the effect of atmospheric pressure and the accompanying convective heat losses on the performance of a vacuum tube collector and to compare the performance of a vacuum tube collector with and without a vacuum. The results of this test are shown in Figure 20. As can be seen in the figure, there was essentially no effect on the heat gain performance with atmospheric pressure inside the collector at low inlet temperatures, i.e., temperatures near ambient; however, as the inlet temperature was raised, convective heat losses became apparent
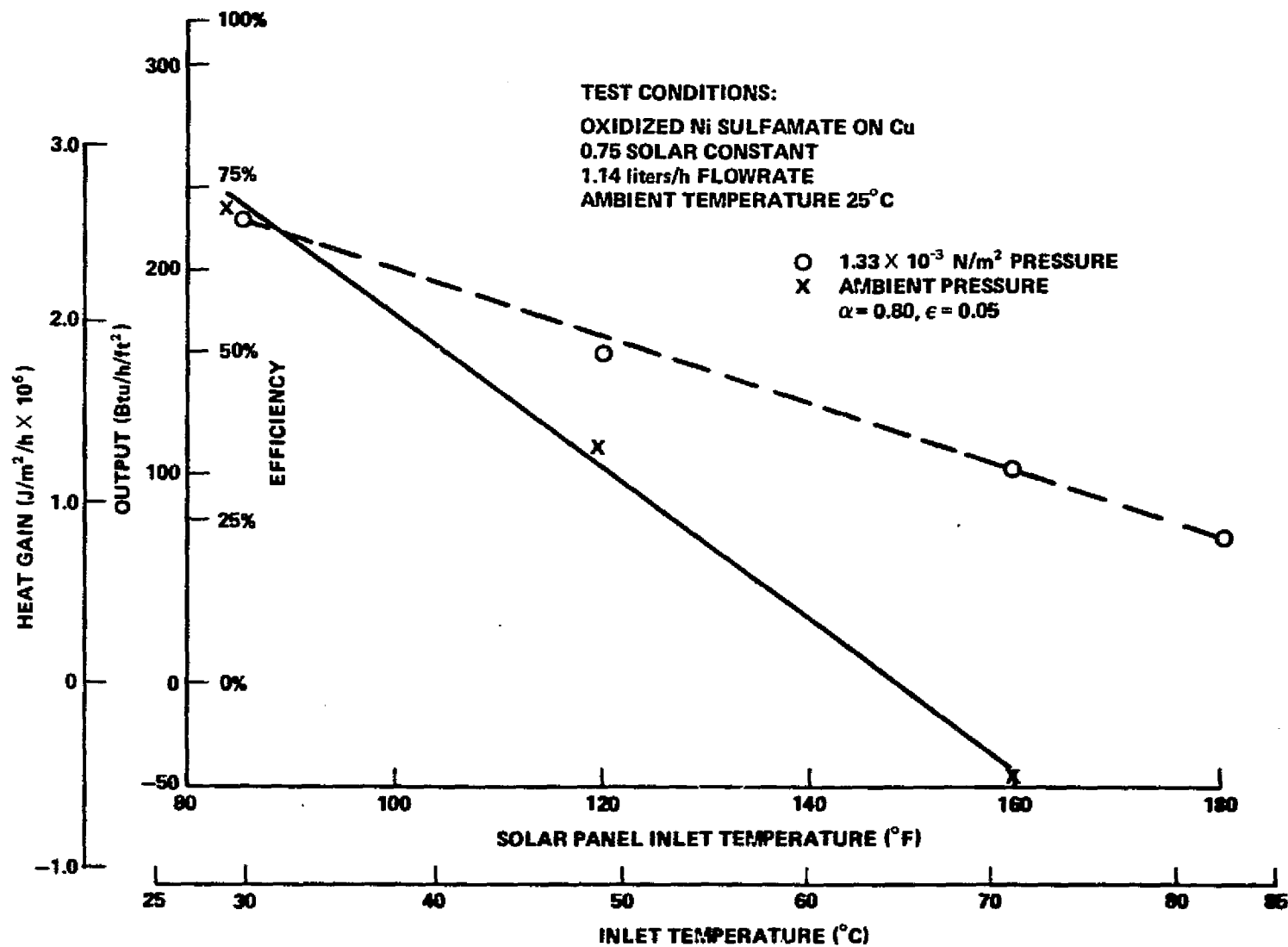
Figure 20. Effect of vacuum insulation on heat gain versus inlet temperature (0.01579 m² replaceable panel evacuated tube collector).

even before 40°C was reached. The net heat gain crossed over from a positive number to a negative number at approximately 65°C. As shown in Figure 20, the presence of atmospheric pressure inside a vacuum tube collector drastically affected its performance at the higher inlet temperatures, even with a selective coating on the collector panel. With a vacuum and an inlet temperature of 65°C, efficiency was approximately 35 percent, whereas without a vacuum, the efficiency had decreased to zero by approximately 65°C.

5. <u>Effect of Reflectors on Heat Gain Versus Inlet Temperature.</u> The purpose of this test was to determine the effect of using reflectors to take advantage of the collector panel backside surface that had been coated during the plating operation, and to establish the characteristic curve shape and its relationship to those in Figure 19 in which no flux intensification had been used. To perform this test, two highly polished aluminum plates were attached to the mounting board behind the glass vacuum tube. One was placed above and the other below the glass tube, as shown in Figure 21.

The polished flat aluminum reflectors had an absorptivity of 0.12 and a reflectivity of 0.88, were 40.6 cm long by 4.76 cm wide, were mounted against the mounting board at one edge, and were set at an approximately 28 degree angle with respect to the mounting board. This resulted in a solar flux incidence angle of approximately 39 degrees with the backside of the collector. The reflector size and mounting angle had been dictated by the distance from the mounting board to the backside of the collector plate. This test setup was definitely not optimized for the use of reflectors; if it had been, the reflectors would have been mounted further behind the collector such that the reflectors could have been larger and the flux incidence angle would have been nearer 90 degrees.

The results of this test are shown in Figure 22. As the figure shows, heat gain was improved considerably even with a less than optimum reflector arrangement. The most noteworthy aspect of this plot is that the improved heat gain curve almost parallels the original nonintensified curve, indicating that this approach certainly merits further investigation where higher operating temperatures are necessary.

6. <u>Effect of Vacuum Insulation on Dry Stagnation Temperature.</u> The purpose of this test was to determine the effect of atmospheric pressure on the dry stagnation temperature of a collector equipped with reflectors, as described in the previous paragraph and shown in Figure 21, and to compare that data with results obtained after a moderate vacuum had been established. The results of this test are shown in Figure 23.

TEST CONDITIONS:

AMBIENT TEMPERATURE 25°C
0.75 SOLAR CONSTANT

TESTS:

1 atm PRESSURE
$1.33 \times 10^{-2}$ N/m² PRESSURE
ZERO FLOW STAGNATION
1.14 liters/h FLOWRATE
HEAT GAIN

39°

INCIDENT ENERGY (TYPICAL)

GLASS ENVELOPE

TEST SPECIMEN

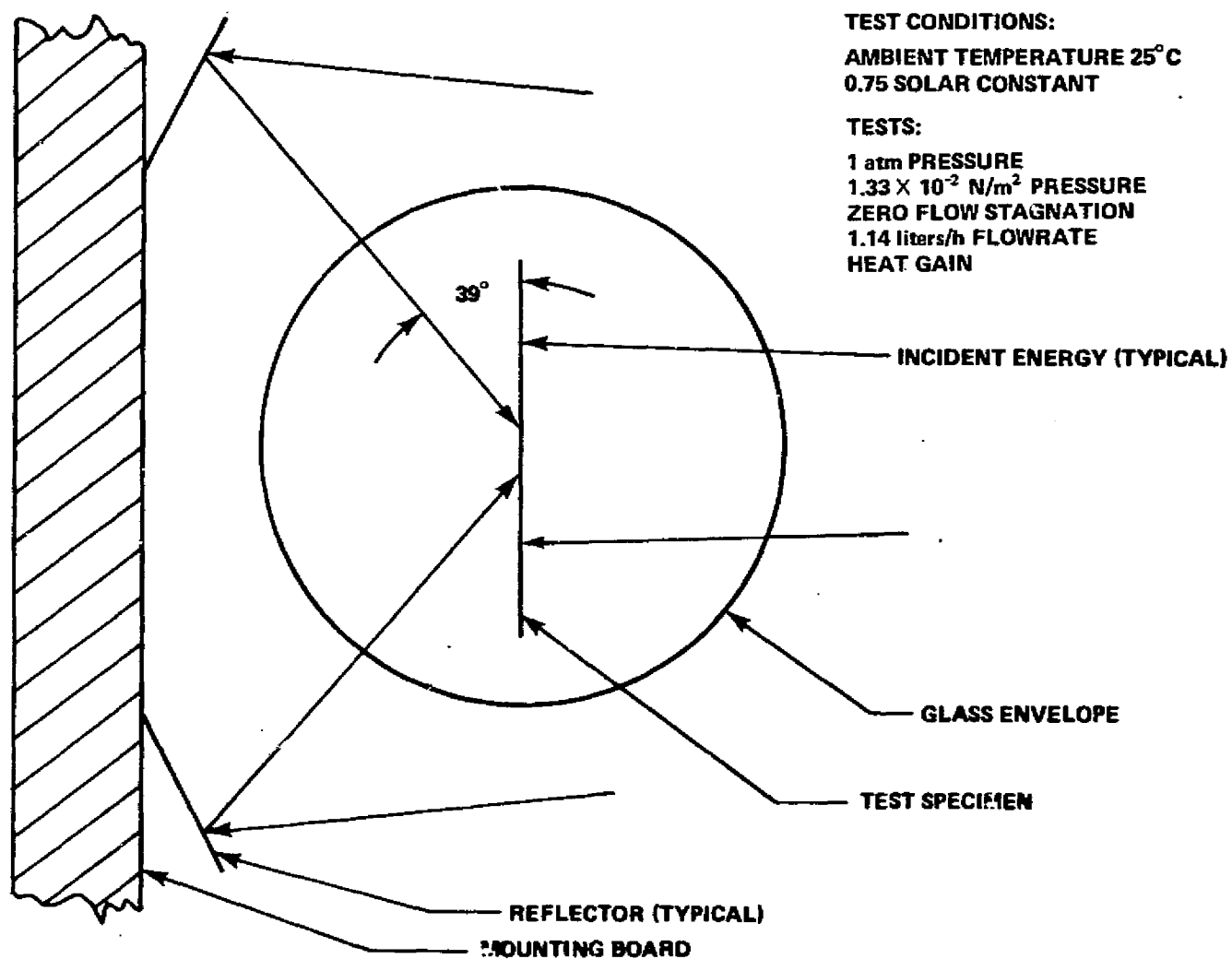REFLECTOR (TYPICAL)

MOUNTING BOARD

Figure 21.   Sketch of reflector test setup used ($0.01579$ m² replaceable
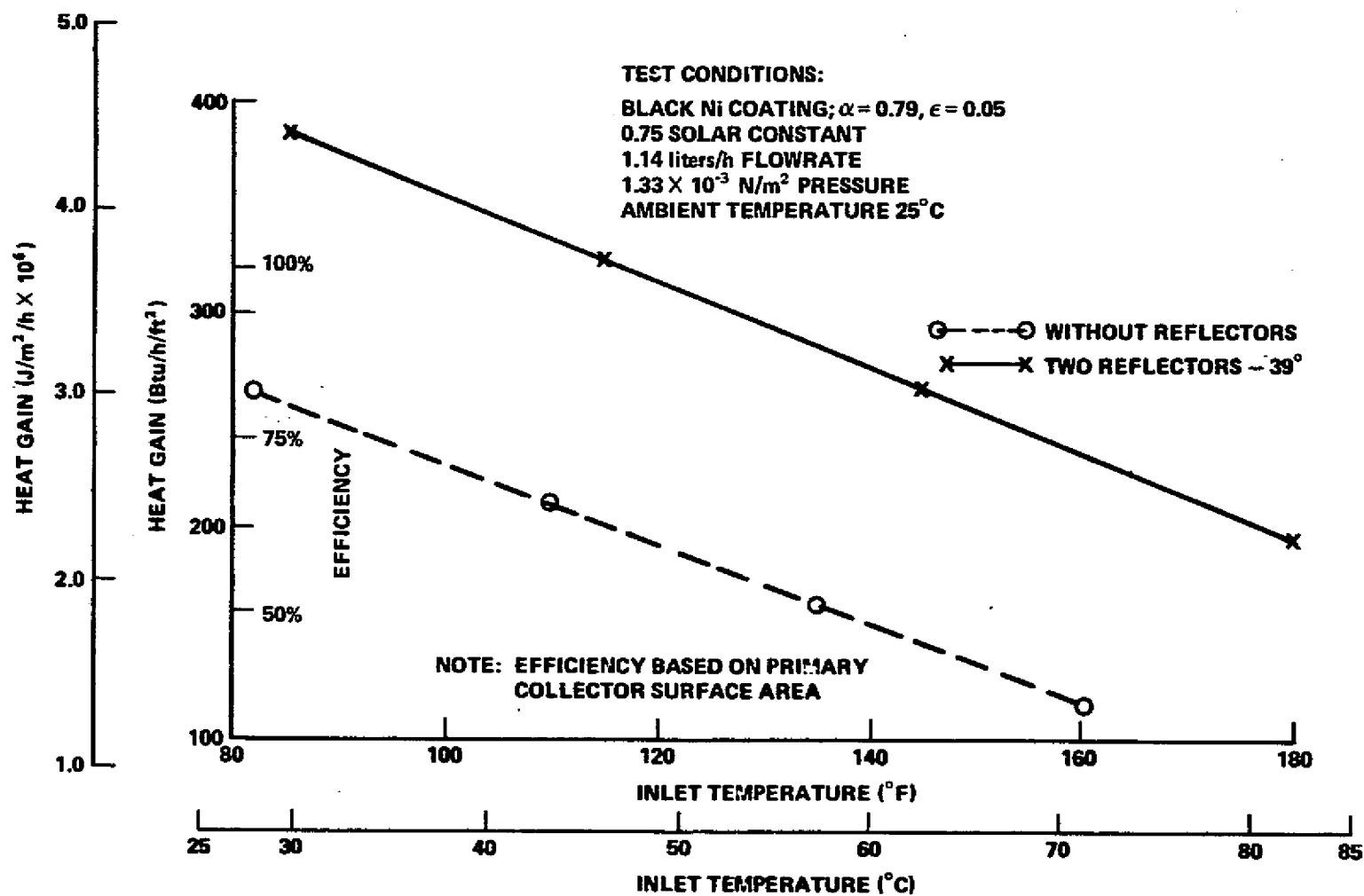panel evacuated tube collector).

Figure 22.   Effect of reflectors on solar collector heat gain $(0.01579 \text{ m}^2$
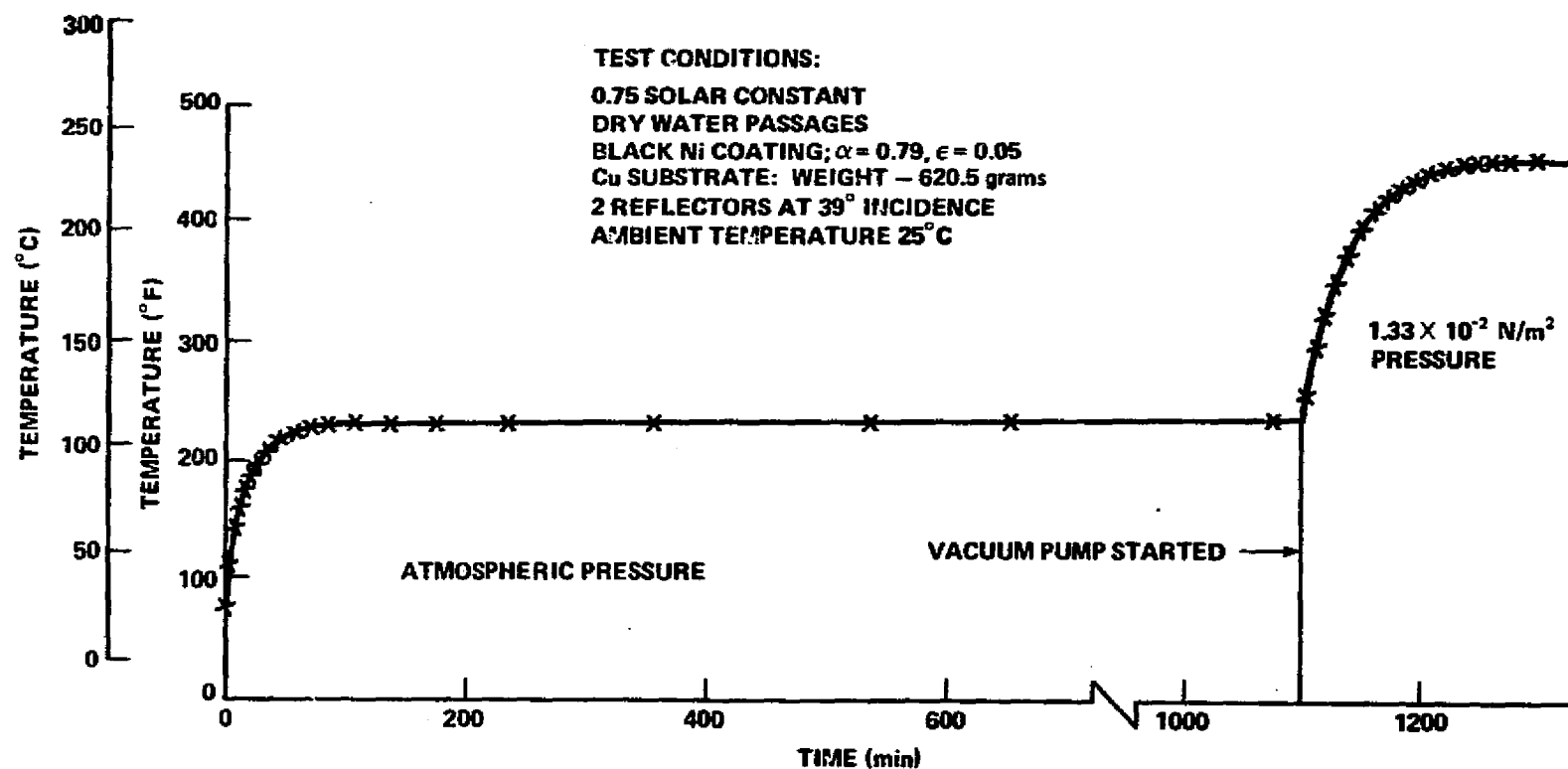Replaceable panel evacuated tube collector).

Figure 23.   Effect of vacuum insulation on dry stagnation temperature
(0.01579 m² replaceable panel evacuated tube collector).

The test was performed as shown, i.e., one continuous run. With atmospheric pressure inside the vacuum tube collector, the collector plate temperature quickly rose to approximately 110°C (230°F) and leveled off at that point. That condition was held for a considerable length of time to assure that steady state conditions had been achieved, and the vacuum pump was started. As Figure 23 clearly demonstrates, the dry stagnation temperature immediately began to rise at a relatively steep rate, slowly leveling off at a new dry stagnation temperature of approximately 233°C (452°F) within 200 min. The same test setup without the reflectors had yielded a stagnation temperature of 194.4°C (382°F). From the data it appeared that optimized reflectors, particularly the curved intensifying type, hold promise for considerably improved performance (heat gain).

## B. Insulated Box Collector

1. <u>Dry Stagnation Tests</u>. As was mentioned in paragraph A.1, the purpose of these tests was to characterize the solar collector design and individual coating and substrate materials. Results of these tests are shown in Table 3 and Figures 24 and 25. Table 3 lists all the coatings and substrate materials tested in the 0.1858 m² (2 ft²) insulated box solar collector and the stagnation temperatures achieved. The stagnation temperatures ranged from 135.6°C (276°F) on the black nickel coated air conditioning condenser coil with the aluminum foil reflector behind it to 152.2°C (306°F) with the P60G2 primer filled with S-28 black pigment on aluminum. It is interesting to note that the stagnation temperature spread was considerably less with the insulated box solar collector than with the vacuum tube type, and the selective coating (black nickel) did not produce nearly as high a stagnation temperature in the insulated box as it had in the vacuum tube collector.

Figure 24 shows a typical selection of dry stagnation temperature curves as a function of time. Those curves shown are considered the maximum, minimum, and typical of all coatings and substrate materials tested to date. Figure 25 shows a change in performance from the first to the second dry stagnation test with the P60G2 primer filled with S-28 black pigment on aluminum substrate. It has been found that the optical properties of this coating change after irradiation. The original absorptivity and emissivity were 0.93 and 0.90, respectively, whereas after exposure they were 0.94 and 0.85, respectively. This characteristic has been noted in several other paints as well. It is

46

## TABLE 3. STAGNATION TEST RESULTS — INSULATED BOX TYPE SOLAR COLLECTOR

| Coating and Substrate | Stagnation Temperature, | |
|---|---|---|
| | °C | °F |
| P60G2 Primer Filled with S-28 Black Pigment, One Coat, Aluminum Substrate | 142.8 152.2 | (289) (306) |
| Black Nickel Coated Air Conditioning Condenser Coil, No Reflector, Open Fins | 146.1 142.8 | (295) (289) |
| Black Nickel Coated Air Conditioning Condenser Coil, Aluminum Foil Reflector Behind Coil | 136.1 135.6 | (277) (276) |
| Black Nickel Coated Air Conditioning Condenser Coil, Fins Bent Closed on Backside (Light Trap) | 142.8 Second Test | (289) Not Run |
| Flat Black (Rustoleum) Paint (Aerosol) on Aluminum (One Coat) | 148.9 142.2 | (300) (288) |
| P60G2 Primer Filled with S-28 Black Pigment, Bonded Aluminum Tubing and Plate | 147.8 150.0 | (298) (302) |
| Caldwell No. C 1077-3 T-Model Black Paint, Aluminum Substrate, Welded Assembly | 142.2 140.6 | (288) (285) |
| Caldwell No. 129-386 Flat Black Paint, Aluminum Substrate, Welded Assembly | 146.7 144.4 | (296) (292) |
| P60G2 Primer Filled with S-28 Black Pigment, Aluminum Substrate, Tube Side Up | 151.1 151.7 | (304) (305) |

Test Conditions

6 kW Solar Simulator
0.75 Solar Constant
Ambient Pressure
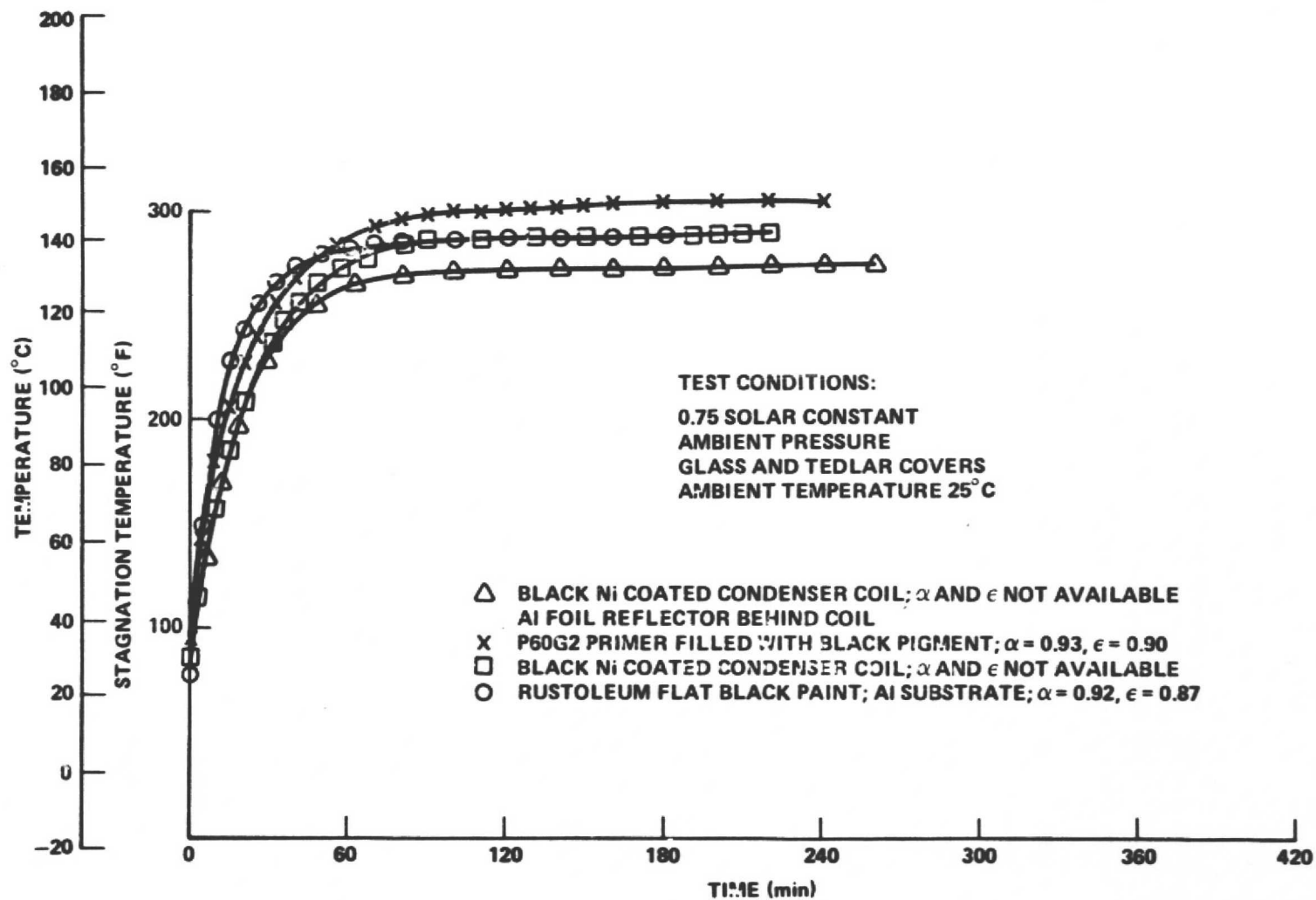Zero Flow Rate
Ambient Temperature of 25°C (77°F)

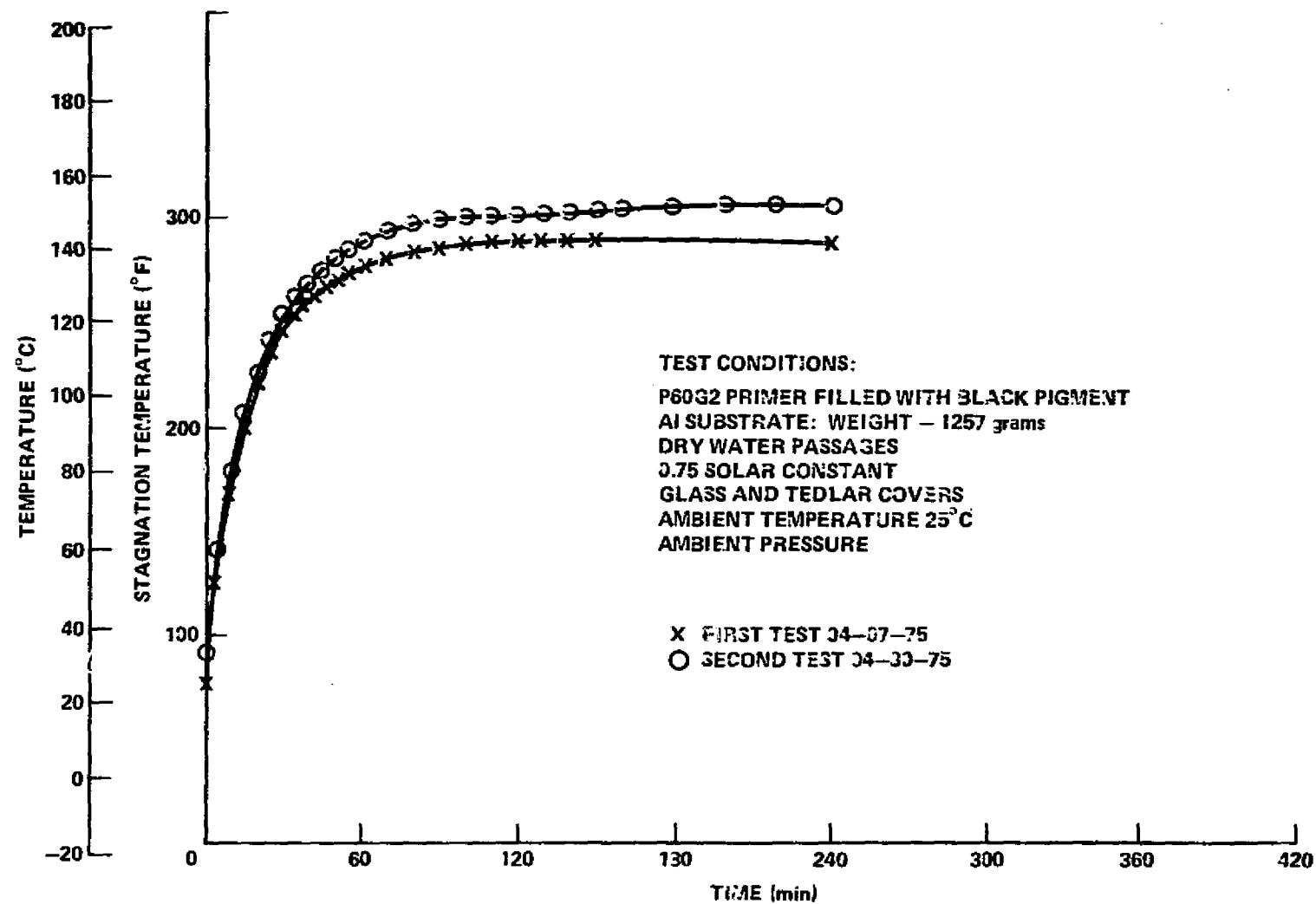Figure 24.  Stagnation temperature comparison (0.1858 m² replaceable panel insulated box collector).

Figure 25. Stagnation temperature comparison for new and aged coating ($0.1858 \, m^2$ replaceable panel insulated box collector).

apparently related to a further curing of the paint. A comparison of the stagnation temperatures of both type collectors (Tables 1 and 3) would indicate that the vacuum tube design is much more sensitive to emissivity. The nonselective coatings (paints) in the vacuum tube collector (Table 1) achieved 106.7° to 115.0°C (224° to 239°F), whereas the selective coatings achieved 161.1° to 194.4°C (322° to 382°F). The insulated box collector appeared to be rather insensitive to emissivity; however, it was more sensitive to absorptivity. The highest temperatures were achieved by the paints, which had the highest absorptivity and, oddly enough, a high emissivity as well. The double glazing on the insulated box design coupled with a covered insulated collector plate backside apparently helped minimize emissivity losses such that absorptivity and convective losses were the controlling heat gain and heat loss factors.

2. Effect of Flow Rate on Heat Gain and Efficiency. The purpose of these tests was to establish a characteristic curve for each coating and substrate such that a flow rate could be selected for the subsequent heat gain as a function of inlet temperature tests that would not penalize the performance of a coating/substrate combination by conducting these tests at an off-nominal flow rate.

Typical results from these tests are shown in Figure 26. As can be noted in Figure 26, flow rates below approximately `. ` liters/h (0.92 gal/h), or 18.8 liters/$m^2$/h (0.46 gal/$ft^2$/h), tended to cause a considerable decrease in heat gain or efficiency. This was related to the fact that as the flow rate went down, water temperature differential across the collector went up causing a higher average plate temperature that resulted in higher heat losses from the collector. It should be noted that these data were taken with relatively low water inlet temperatures.

Although the flow rates with the insulated box collector differ from those discussed concerning the 0.01579 $m^2$ (0.17 $ft^2$) evacuated tube collector, the discussion of results is generally the same. The flow rate selected for subsequent tests was a tradeoff, i.e., a flow rate high enough that low inlet temperature performance did not suffer unduly but low enough such that collector temperature differential, heat gain, at high water inlet temperatures did not drop below a useful value. This useful value would probably depend on total system performance, water pumping costs, heat losses through the system, etc. As noted from Figure 26, only four of the nine coating/substrate configurations were plotted on the curve. The reason for this was that the other black nickel coated air conditioning condenser coil curves fell almost exactly over the one plotted, and data from the other black paints tested fell almost
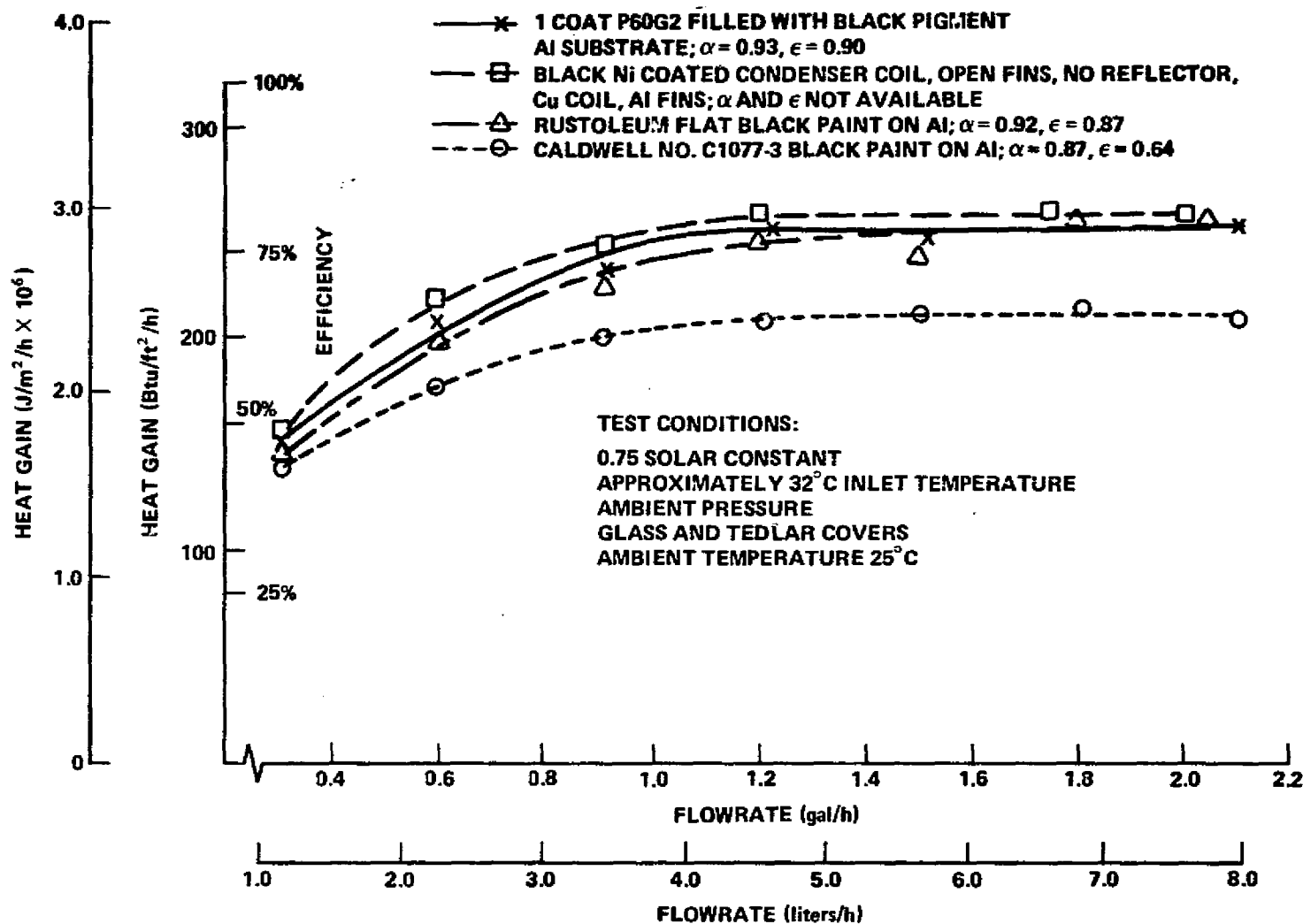
Figure 26. Effect of flow rate on heat gain and efficiency (typical 0.1858 m²
replaceable panel insulated box collectors).

exactly over the curve of the Sherwin-Williams P60G2 primer filled with Sheppard S-28 black pigment. For subsequent heat gain as a function of inlet temperature tests, a water flow rate of 30.56 liters/$m^2$/h (0.75 gal/$ft^2$/h) was utilized.

3. <u>Effect of Inlet Temperature Change on Heat Gain as a Function of Flow Rate</u>. The purpose of these tests was to establish the characteristic curve shape for the heat gain as a function of flow rate at a low inlet temperature, approximately 32°C (90°F), and at a high temperature, approximately 82°C (180°F), in order that a family of curves could be interpolated for inlet temperatures other than those where the tests were conducted. It was believed that these curves and data would be beneficial in understanding solar collector performance characteristics and design tradeoffs that would be required to optimize these parameters in an operating system. The results of these tests are plotted in Figure 27. The heat gain curve generated for an inlet temperature of approximately 32°C (90°F) is the same as that shown in Figure 26; therefore, the same analysis and comments apply. The collector inlet and outlet temperaure differential and heat gain is shown with each data point to permit a better understanding of the relationships involved (Fig. 27).

The curve plotted from data taken at approximately 82°C (180°F) revealed a considerable drop in heat gain performance as a result of the increase in inlet temperature. The decrease in performance is undoubtedly the result of increased heat losses as a result of the higher average collector plate operating temperature. The shape of the curve generated from the higher temperature data is similar to the lower temperature data curve; further, both curves show a slight decrease in performance and efficiency as the water flow rate was decreased below approximately 6 liters/h (1.6 gal/h). Ever decreasing performance and efficiency were noted at lower flow rates.

4. <u>Effect of Inlet Temperature on Heat Gain</u>. The purpose of testing each candidate coating/substrate in this fashion was to obtain quantitative data on the ability of this collector design and each coating, coating/substrate, or coating/absorber plate configuration to convert solar type radiation into usable heat energy over a range of inlet temperatures in an operating system. In an operating hot water system, the reservoir temperature would slowly rise with several days of bright sunshine. The data presented in Table 4 and Figure 28 give an indication of the heat energy that might be collected per unit area at the collector with collector water inlet temperatures as shown, a solar intensity of 0.75 solar constant, a beam energy normal to the collector surface, and an
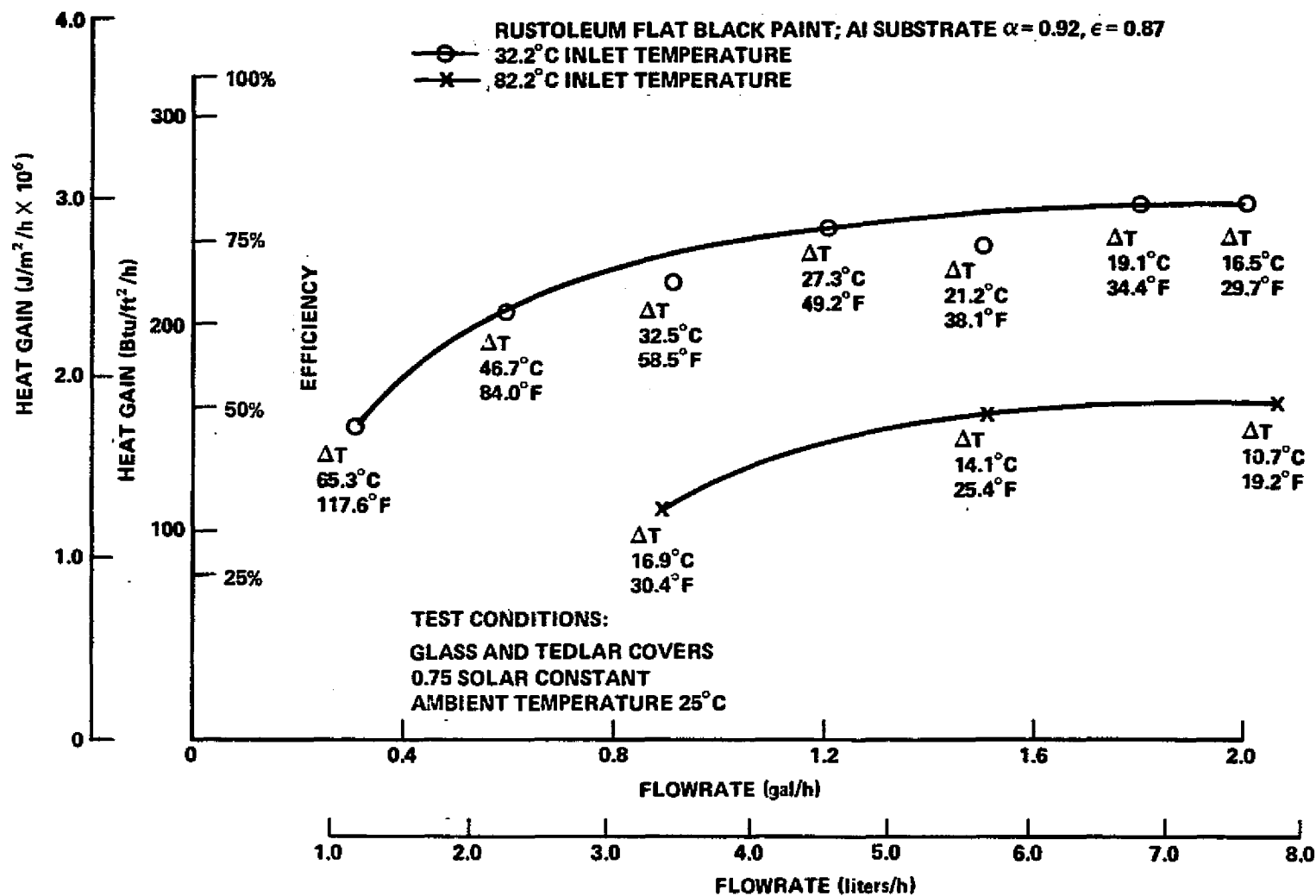
Figure 27. Effect of inlet temperature change on heat gain versus flow rate (0.1858 m² replaceable panel insulated box collector).

| Coating and Substrate | Gain Heat, $J/m^2/h \times 10^6$ (Btu/ft$^2$/h) | | | | | | | |
|---|---|---|---|---|---|---|---|---|
| | 35°C | (95°F) | 48.9°C | (120°F) | 71.1°C | (160°F) | 82.2°C | (180°F) |
| P60G2 Primer, S-28 Pigment, Aluminum Substrate, $\alpha = 0.93$, $\epsilon = 0.90$ | 2.80 | (246.5) | 2.66 | (234.3) | 2.23 | (196.1) | 1.93 | (170.0) |
| Black Nickel Coated Air Conditioning Condenser Coil, $\alpha$ and $\epsilon$ Not Available | 2.83 | (248.9) | 2.73 | (240.3) | 2.30 | (202.1) | 2.00 | (175.7) |
| Black Nickel Coated Air Conditioning Condenser Coil, Aluminum Foil Reflector | 2.92 | (257.3) | 2.72 | (239.9) | 2.26 | (199.2) | 1.89 | (166.7) |
| Black Nickel Coated Air Conditioning Condenser Coil, Bent Fins (Light Trap) | 2.88 | (253.4) | 2.72 | (239.6) | 2.32 | (204.3) | 2.22 | (195.5) |
| Rustoleum Flat Black Paint, Aluminum Substrate, $\alpha = 0.92$, $\epsilon = 0.87$ | 2.70 | (237.4) | 2.71 | (238.6) | 2.26 | (199.2) | 1.79 | (157.2) |
| P60G2 Primer, S-28 Pigment, Aluminum Substrate, Bonded Assembly, $\alpha = 0.94$, $\epsilon = 0.85$ | 2.65 | (233.6) | 2.43 | (213.7) | 2.01 | (177.2) | 1.84 | (162.3) |
| Caldwell No. C 1077-3 Flat Black Paint, Aluminum Substrate, $\alpha = 0.87$, $\epsilon = 0.64$ | 2.40 | (211.4) | 2.16 | (190.6) | 1.82 | (160.0) | 1.52 | (133.8) |
| Caldwell No. 129-386 Flat Black Paint, Aluminum Substrate, $\alpha = 0.92$, $\epsilon = 0.87$ | 2.99 | (263.3) | 2.50 | (219.9) | 2.22 | (195.3) | 2.02 | (177.8) |
| P60G2 Primer, S-28 Pigment, Aluminum Substrate, Tube Side Up, $\alpha = 0.94$, $\epsilon = 0.85$ | 2.92 | (257.4) | 2.52 | (221.7) | 2.18 | (192.2) | 1.93 | (170.0) |

Test Conditions

6 kW Solar Simulator
0.75 Solar Constant
5.68 liters/h (1.5 gal/h) Flow Rate, 30.56 liters/m$^2$/h (0.75 gal/ft$^2$/h)
Ambient Pressure
Ambient Temperature of 25°C (77°F)

TABLE 4. HEAT GAIN VERSUS INLET TEMPERATURE TEST RESULTS — 0.1858 m$^2$ (2 ft$^2$) INSULATED BOX COLLECTOR WITH VARIOUS SOLAR PANELS
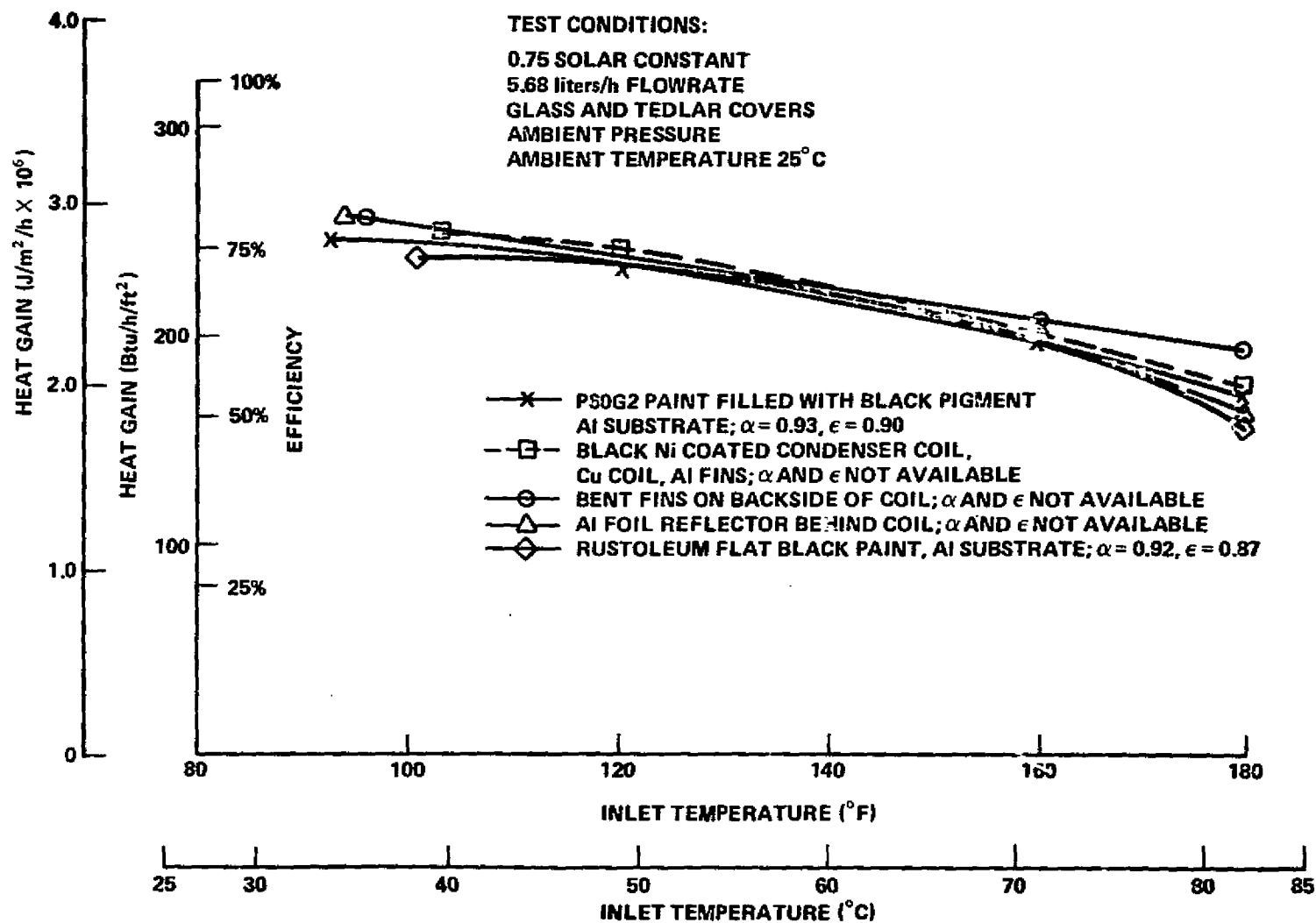
Figure 28.   Effect of inlet temperature on heat gain (0.1858 m² replaceable panel insulated box collector).

ambient temperature of 25°C (77°F). A solar intensity of 0.75 solar constant, a beam energy normal to the collector surface, and an ambient temperature of 25°C were chosen such that collected heat energy data would reflect the highest values that could normally be expected in northern Alabama. For solar intensities less than those used for these tests, solar beam energy incidence angles less than 90 degrees, or ambient temperatures other than 25°C, calculations would be needed to determine the expected output.

An analysis of the data shown in Figure 28 and Table 4 would indicate that data from all tests tended to fall in a more tightly clustered group with the insulated box collector than with the vacuum tube collector configuration, except for the Caldwell No. C 1077-3 black paint which performed poorly compared to the other coatings. Correlation of the low inlet temperature heat gain data with absorptivity and emissivity numbers showed that the highest performers were the coatings with high absorptivity. These included, for instance, the Caldwell No. 129-386 with an absorptivity of 0.92 and an emissivity of 0.87, P60G2 primer on aluminum with S-28 pigment added with the tube side of the panel toward the simulator and with an absorptivity of 0.94 and an emissivity of 0.85, and the selective black nickel coated air conditioning condenser coil. Unfortunately, the surface of the air conditioning condenser coil did not lend itself to an optical properties check; therefore, these values are not available.

Analysis of data from the insulated box collector tests completed to date indicated that absorptivity is the overriding parameter in coating heat gain performance with this configuration collector, at least up to the temperatures achieved in these tests. Emissivity would become an increasingly important factor at higher collector temperatures. These test data show that the best coating for use in the insulated box collector at temperatures up to 82.2°C (180°F) would be one with the highest possible absorptivity with little regard for emissivity, possibly a low priced paint.

The intended use of the insulated box collector at temperatures above some point, 93°C (200°F) for instance, might warrant consideration of a more sophisticated plate design such as a light trap plate configuration; however, since Table 3 revealed a stagnation temperature of 142.8°C (289°F) for this configuration, this collector design's usefulness probably would not extend very far past the 100° to 110°C (212° to 230°F) range, possibly as high as 125°C (257°F). It is obvious that useful heat gain performance cannot extend completely to dry stagnation temperature.

At the intermediate temperatures, the performance of almost all the collector plates/coatings were similar (Table 4), except the Caldwell No. C 1077-3 and the plate that had been thermally bonded to the tubing. A check of the data on this plate/coating revealed that the temperature differential between the collector plate and the plate discharge water was approximately twice as great as that of the plates which had been brazed/welded at assembly.

Correlation of the high inlet temperature heat gain data with absorptivity and emissivity showed that the higher absorptivity coatings generally performed better, except the Caldwell No. C 1077-3 and the thermally bonded plate-to-tube assembly. The Rustoleum flat black paint performance fell rather sharply at the 82.2°C (180°F) inlet temperature test point. It was also noted that the light trap version of the black nickel coated air conditioning condenser coil began to show considerable performance margin over the other coatings and configurations at the 82.2°C (180°F) test point. The light trap configuration, not necessarily the finned coil version, might well be an attractive plate configuration for an insulated box collector intended for higher temperature service.

As noted in Table 4, the Caldwell No. C 1077-3 gloss black paint was the poorest performer by a considerable margin at the 82.2°C (180°F) test point. The fact that its emissivity was considerably lower than that of the other paints, 0.64 as compared to 0.85 to 0.90 with the other paints, failed to offset the performance differences caused by the lower absorptivity of the C 1077-3, 0.87 as compared to 0.92 to 0.94 with the other paints.

5. Heat Gain Performance Comparison Between Brazed and Thermally Bonded Collector Plate to Tube Assembly Methods. The purpose of this test was to evaluate a thermal bonding compound versus a brazed assembly from the standpoint of heat gain performance. The decision to test a thermal bonding compound was a result of problems that had been encountered in brazing the aluminum tubes to the plates. The problems were associated with maintaining a metal-to-metal contact between the tube and plate over its entire length during the heating, brazing, and cooling cycle in order to obtain a good braze joint the full length of the tube. Several different methods were utilized in brazing the tubing to aluminum plates; furnace brazing, a temperature controlled hot plate, and a gas torch. Each method presented difficulties; therefore, the decision was made to test an alternate assembly technique, a thermal bonding compound. The compound used was Hysol 934, epoxy heavily filled with aluminum filings.

The results of these tests are shown in Table 4 and Figure 29. The brazed assembly performed better than the thermally bonded assembly by $9.0 \times 10^4$ to $2.3 \times 10^5$ J/m$^2$/h (2.4 to 6.4 percent). This was considered a significant reduction in heat gain performance; consequently, no further tests were made on the thermally bonded assembly.

6. <u>Comparison of Vacuum Tube Versus Insulated Box Heat Gain as a Function of Inlet Temperature.</u> Figure 30 compares the data taken from tests of these two collector system concepts utilizing a common coating, substrate, and collector plate assembly method. The collector plate tested in both collector system concepts used the Rustoleum flat black paint on aluminum substrate with aluminum tubing brazed to the plate. As can be observed, the heat gain of the small 0.01579 m$^2$ (0.17 ft$^2$) vacuum tube collector decreased much more rapidly with increasing inlet temperature than did that of the 0.1858 m$^2$ (2.0 ft$^2$) insulated box collector. As was discussed previously, this rapid decrease in heat gain performance with the vacuum tube collector was thought to be a result of conductive heat losses through the tubing being an appreciable percentage of the total heat gain involved, since the solar panels being tested were small in area. It can also be noted that the heat gain performance of the small vacuum tube collector at low inlet temperatures was considerably higher than that of the insulated box configuration collectors. (See Figures 19 and 28 for other coating comparisons.) This characteristic was attributed to the fact that the vacuum tube collector had one glass cover, whereas the insulated box collector had two covers, one glass, and the other Tedlar plastic film and to the fact that the area of the Rustoleum flat black painted panel was approximately 6 percent oversized as compared to the other samples.

With an assumed transmissivity of 0.92 for the Pyrex glass tube of the small evacuated tube collector and coating absorptivities as shown in Figure 19, the low inlet temperature heat gain efficiencies of the coatings on the two collectors mathematically should have ranged from 73 to 86 percent with some nominal variance for measurement errors.

## C. Insulated Box Collector Tested in Sunlight

The purpose of this test was to compare the dry stagnation temperature and the heat gain performance as a function of inlet temperature results gained from solar simulator tests with those obtained from actual sunlight. The test apparatus was moved outdoors for these tests. No changes were made in the
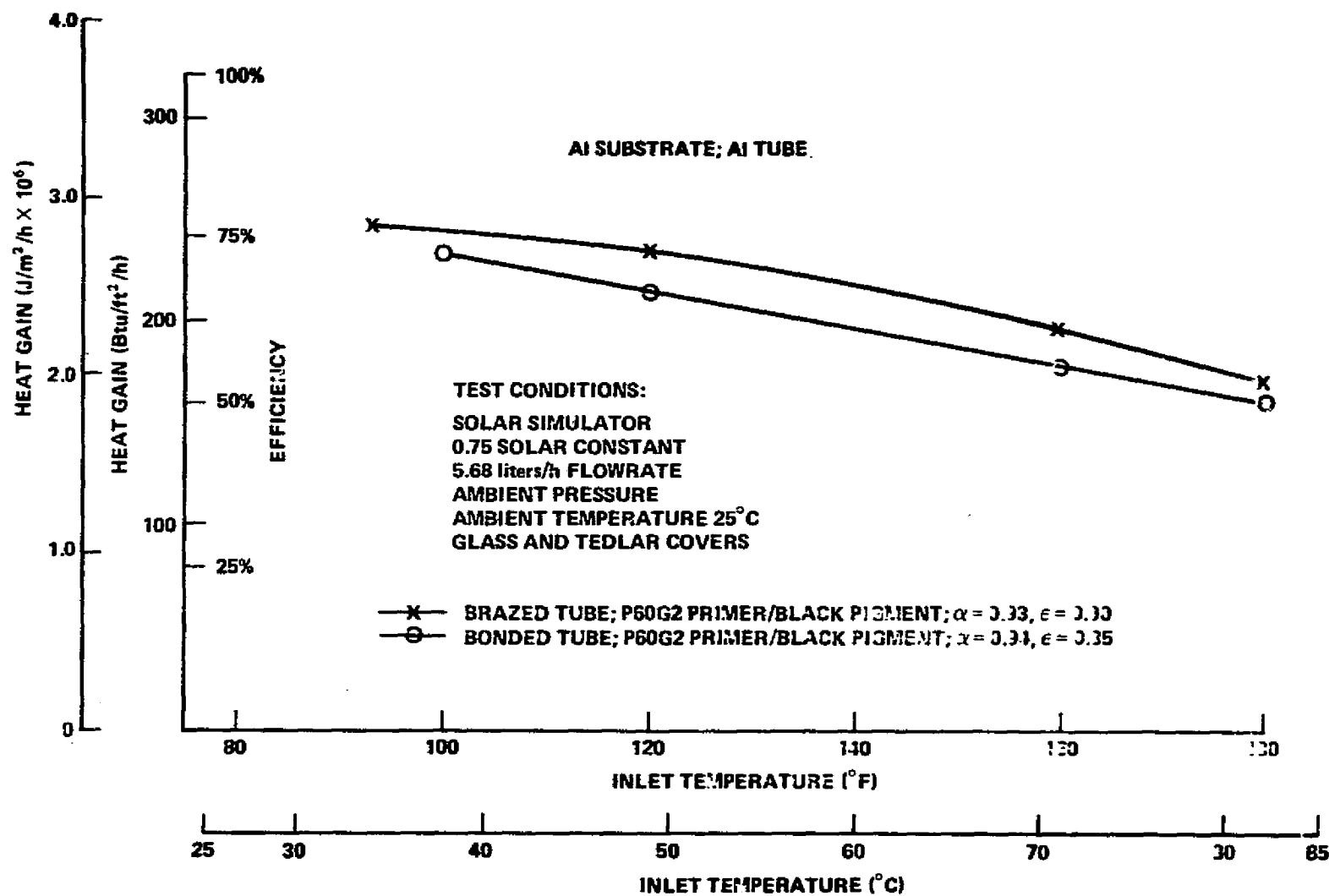
Figure 29. Heat gain versus inlet temperature for brazed versus bonded tube-to-plate (0.1858 m² replaceable panel insulated box collector).
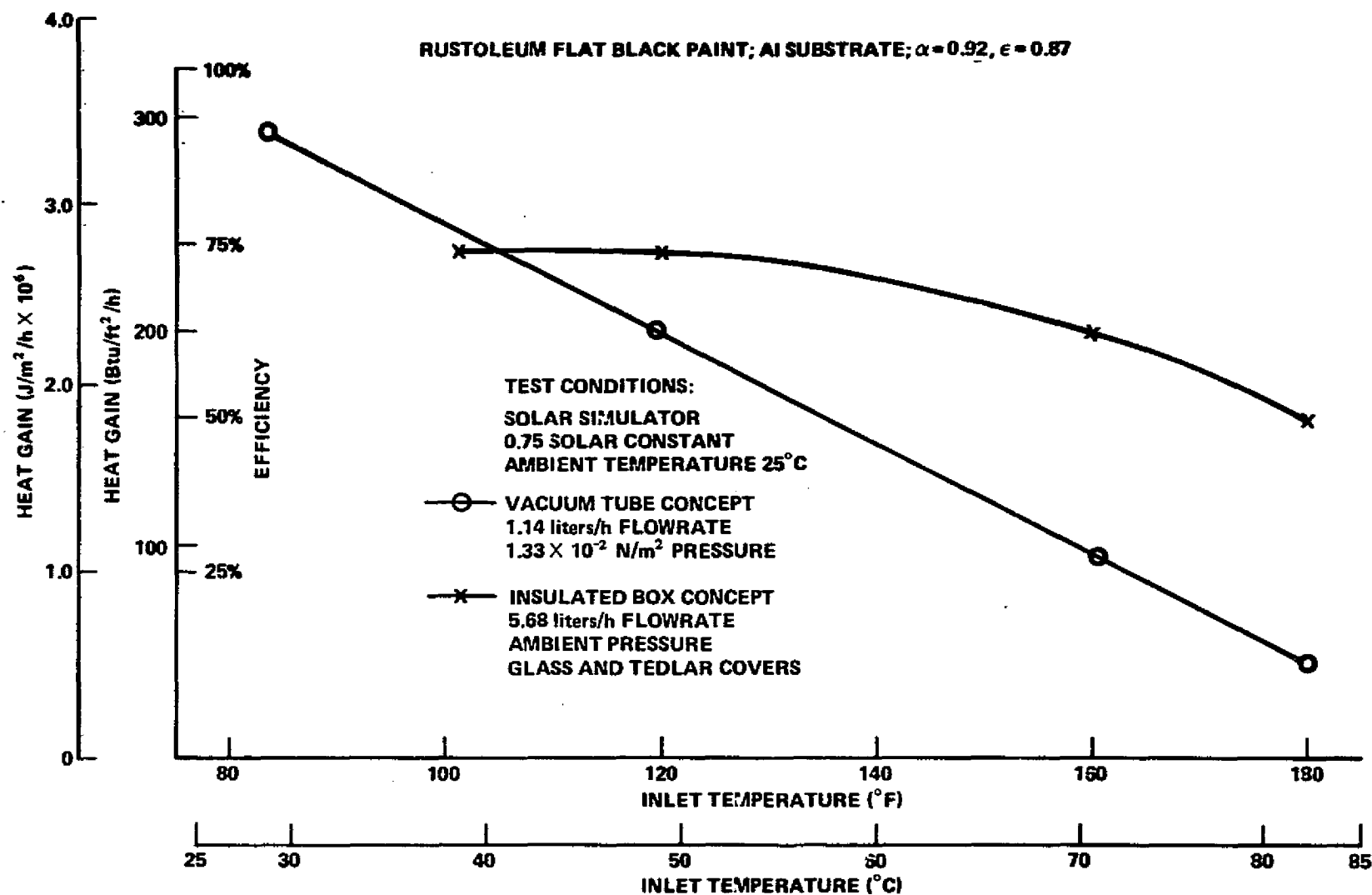
Figure 30.   Comparison of replaceable panel vacuum tube $(0.01579\ m^2)$
and replaceable panel insulated box collectors $(0.1858\ m^2)$.

test setup. The collector was positioned south facing such that it would be normal to the Sun at solar noon. The collector and pyrheliometer were left stationary in that position for each test, which lasted from approximately 8:00 a.m. to 4:00 p.m., weather permitting. Figure 12 shows this collector.

1. Dry Stagnation Test. The dry stagnation temperature achieved during this test was 127.8°C (262°F) with an insolation of approximately 0.65 solar constant. It should be noted that complete equilibrium had not been achieved when a cloud drifted across the Sun reducing the insolation value considerably. Assuming a linear function between solar insolation value and dry stagnation temperature, with a 23.9°C (75°F) stagnation temperature at zero insolation and a 127.8°C (262°F) stagnation temperature at 0.65 solar constant, a 0.75 solar constant would yield a 143.8°C (290.8°F) stagnation temperature. Figure 31 is a graphical representation of this normalization curve. A 127.8°C (262°F) stagnation temperature at 0.65 solar constant is considered a relatively close correlation to the 151°C (304°F) which had been experienced after approximately 4 h at 0.75 solar constant with the solar simulator, particularly since equilibrium was not achieved in the actual sunlight test.

2. Heat Gain as a Function of Inlet Temperature Tests. The data obtained from heat gain versus inlet temperature tests made in actual sunlight are shown in Figure 32. Also plotted for comparison purposes are data from the same collector utilizing the solar simulator as the source. The actual sunlight and solar simulator curves are in close agreement at the high inlet temperature end of the curve; however, at the low inlet temperature, data from the actual sunlight tests indicate a higher heat gain.

The only known explanations for this variation have to do with the ambient temperatures of the test areas, the wind velocity during tests outside, the spectral intensity of solar radiation versus that of the solar simulator xenon lamp, and the spectral absorptivity of the collector covers and the solar collector coating, i.e., P60G2 primer filled with S-28 black pigment. Solar radiation intensity is higher in the shorter wavelengths, 0.4 to 0.75 $\mu$m, and xenon lamp radiation is more intense in the infrared range, 0.75 to 1.1 $\mu$m (the xenon lamp is known to be rich in infrared). The solar collector coating absorptivity would also be expected to vary with temperature or radiant energy wavelength. Therefore, the significance of this difference could only be determined by comparing coating spectral plots with intensity versus wavelength plots of solar radiation and simulator output. The solar simulator tests were made inside a building with a relatively constant ambient temperature of approximately 25°C (77°F)

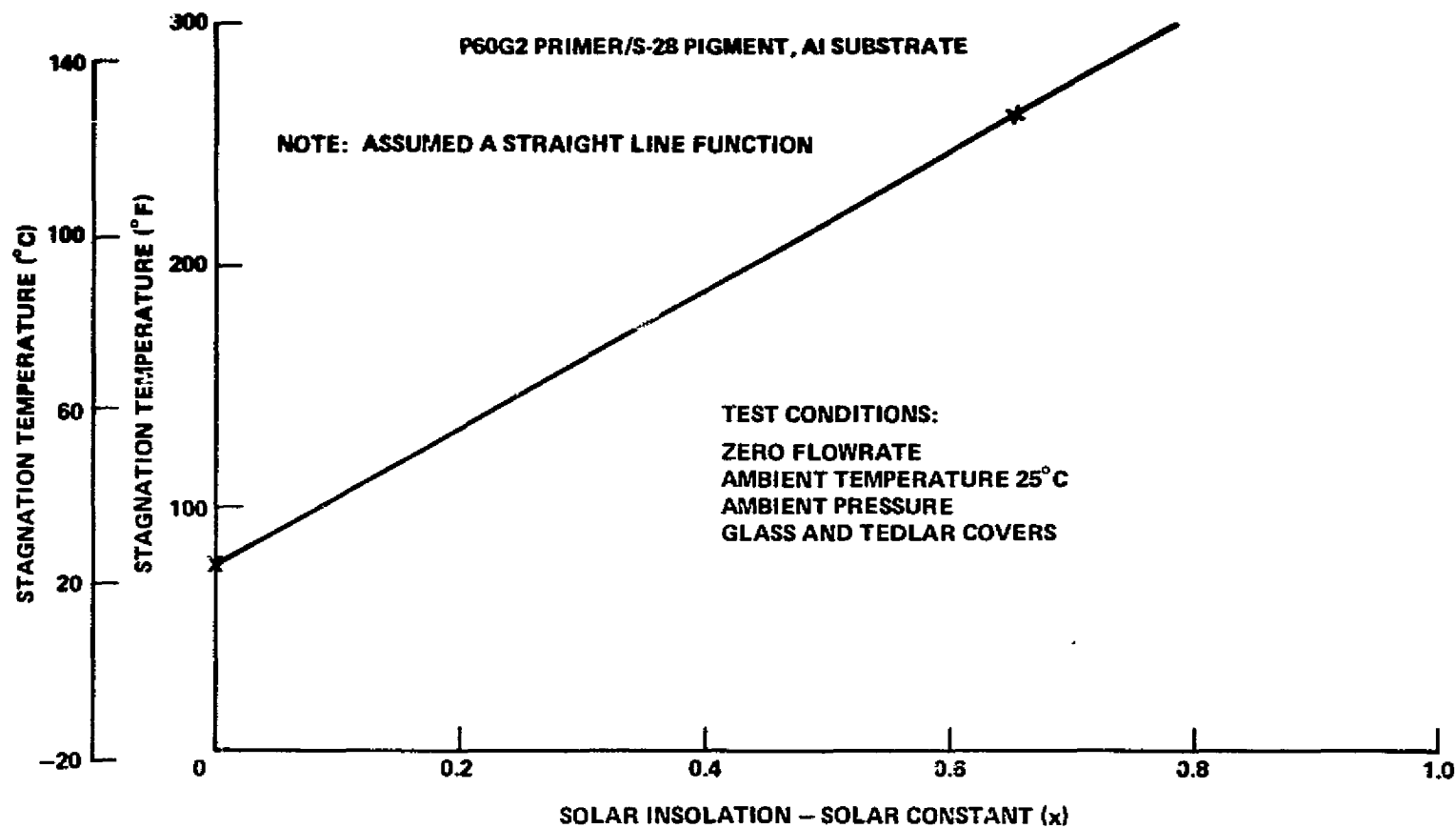Figure 31.   0.1858 m² replaceable panel insulated box collector stagnation temperature as a function of insolation.
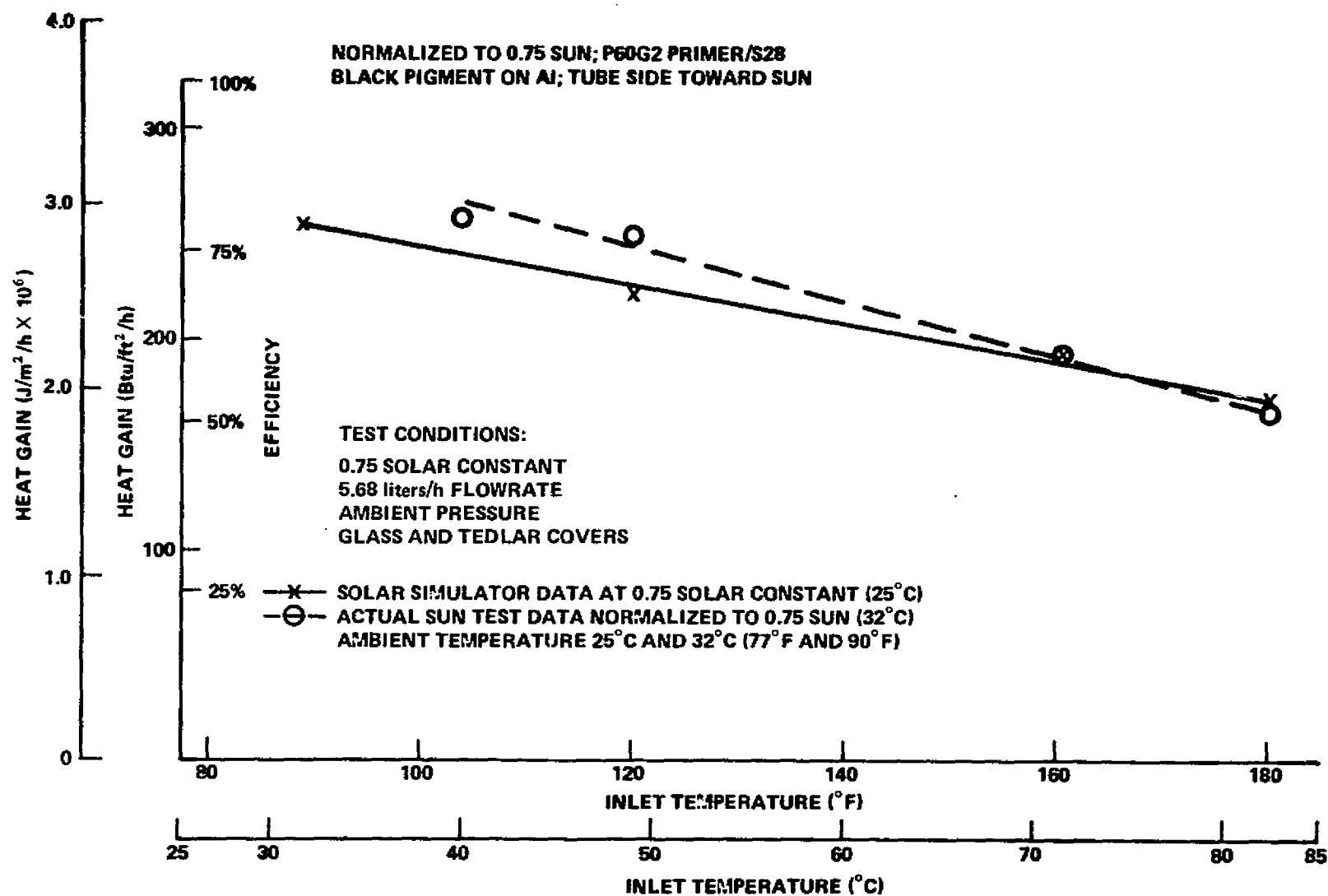
Figure 32.   0.1858 m² replaceable panel insulated box collector heat gain versus
inlet temperature (solar simulator versus sunlight).

and no wind, whereas the actual sunlight tests were performed outside where the ambient temperature was approximately 32°C (90°F). No wind velocity measurements were made. Assuming that ambient temperature is a correct explanation, it is interesting that the higher ambient temperature did not affect the data substantially at the higher inlet temperatures; however, the wind could have affected that data. In general, it was considered that solar simulator data were representative of actual sunlight data.

## D. Sealed Tube Evacuated Collector in Sunlight

The purposes of these tests were to determine whether there was a "sc. ing factor" type difference in heat gain versus inlet temperature performance between this $0.081$ m$^2$ ($0.875$ ft$^2$) collector and the $0.01579$ m$^2$ ($0.17$ ft$^2$) collector discussed previously, and to permit a heat gain performance comparison between actual sunlight and a xenon lamp solar simulator utilizing this sealed tube collector. This assembly has not as yet been tested utilizing a solar simulator.

1. **Dry Stagnation Test.** The purposes of this test were to assist in characterizing this solar collector and the solar collector coating used on the absorber panel, and to compare the stagnation temperature of this collector in actual sunlight with that achieved when the unit is tested with a solar simulator. The only change made to the test equipment for this test was to remove the insulated box collector and install the sealed tube evacuated collector. The temperature sensing thermocouples were installed into the water flow path tubing to sense the tube (and plate) temperature for this test only. The thermocouples were installed at different depths for a better sampling of plate temperature. One was installed far enough to be at the turnaround bend in the tubing. The tubing was sealed around the thermocouple wire to prevent convection cooling inside the tubing. The collector was positioned south facing such that it would be normal to the Sun at solar noon. The collector and pyrheliometer remained stationary in that position for the entire test. The dry stagnation temperature achieved by this collector in actual sunlight was 156.1°C (313°F) at 0.52 solar constant. Since this collector has not been tested utilizing a solar simulator, no data comparison can be made. However, if the same assumption can be made as was made concerning stagnation temperature being a linear function with insolation, an equivalent dry stagnation temperature can be calculated by establishing 32.2°C (90°F) as the stagnation temperature with zero insolation and 156.1°C (313°F) at 0.52 solar constant as another point on the curve. If

this assumption is made, the dry stagnation temperature at 0.75 solar constant would be 210.9°C (411.6°F). It should be noted that Table 1 listed the black nickel coated copper panel in the small evacuated tube collector as having achieved a 194.4°C (382°F) dry stagnation temperature at 0.75 solar constant utilizing a solar simulator.

2. Heat Gain as a Function of Inlet Temperature Tests. The purposes for these tests were to provide data in order that comparisons could be made between the heat gain performance at two different water flow rates, the heat gain performance of the small 0.01579 m² (0.17 ft²) evacuated tube collector and the larger 0.081 m² (0.875 ft²) sealed tube evacuated collector, and the heat gain performance of this collector in actual sunlight and its performance when tested with a solar simulator source. Again, it should be noted that the 0.081 m² (0.875 ft²) sealed tube evacuated collector has not been tested utilizing a solar simulator source.

The only changes made for this test were to remove the thermocouples from the collector water flow path and to flow through the collector in preparation for the test. The collector was positioned south facing such that it would be normal to the Sun at solar noon. The collector and pyrheliometer remained stationary in that position for each entire test. A portion of the data taken from these tests is shown in Figure 33. The data used in plotting these curves were taken from test days when solar intensity was the highest and when the Sun was at or near (plus or minus 1 h) solar noon, such that Sun angles and normalization of data to 0.75 solar constant would introduce a minimum of error into the data. As shown in Figure 33, the higher flow rate, 69.27 liters/m²/h (1.7 gal/ft²/h), yielded higher heat gain performance numbers than did the lower flow rate. The reasons for this have been discussed previously. In general, heat gain performance varied from approximately 87 percent efficiency at 21°C (70°F) to approximately 53 to 54 percent efficiency at 82°C (180°F). This performance was due to collector absorption on the front side only; black construction paper was used in back of the collector to minimize, as much as possible, collector backside absorption, since both sides of the collector plate were coated with black nickel. Tests performed without the black construction paper in place yielded efficiencies of approximately 100 percent at a 30°C inlet temperature based on front side radiation area. Apparently there was sufficient reflection from the plywood mounting board (background) to increase heat gain performance by approximately 16 percent at the 30°C inlet temperature data point. Heat gain performance numbers in this report are based on absorber plate area rather than collector overall area. As a result of tests on this unit
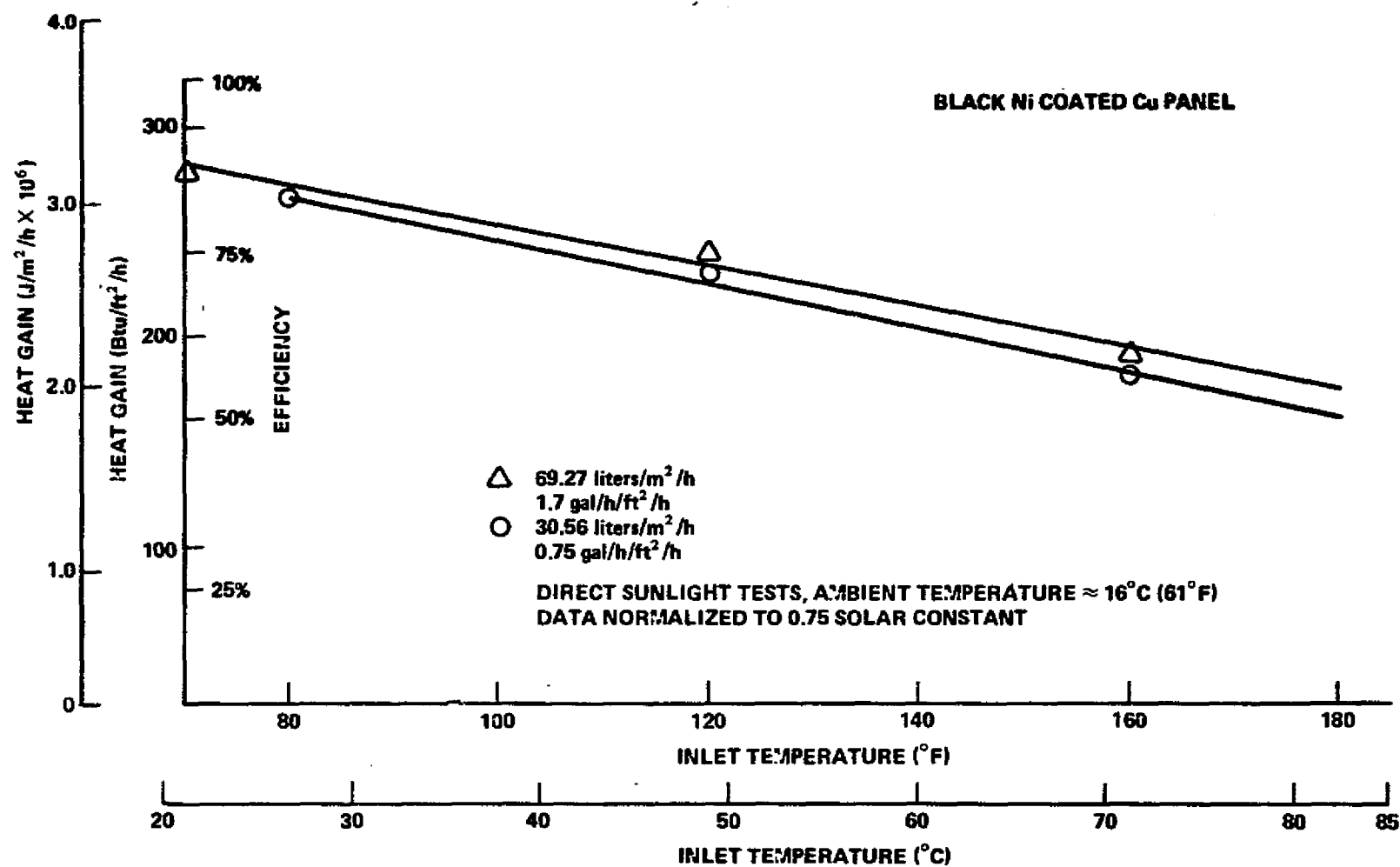
Figure 33. Heat gain versus inlet temperature for two flow rates
(0.081 m² sealed tube evacuated collector).

and the small 0.01579 m$^2$ (0.17 ft$^2$) evacuated tube collector with reflectors, it appears that considerably increased performance would be possible with an optimized system of vacuum insulated collectors and concentrating reflectors. It might be particularly attractive where reservoir temperatures in excess of 94°C (200°F) are required.

3. <u>Solar Intensity, Sun Angle, and Heat Gain as a Function of Time.</u> The purpose of this test was to establish the characteristic curve shapes of Sun angle, solar intensity, and heat gain over a day long test with a stationary collector, without reflectors, and with a constant flow rate and inlet temperature. No test setup changes were made for this test; however, measurements of the solar incidence angle with respect to the collector plate were made and recorded periodically throughout the day. The data taken during this test are shown in Figure 34. The data chosen for this chart were taken from a day when the weather was clear, after the passage of a cold front.

The data plotted on the graph show that the Sun angle with respect to the collector plate was a linear function with time; the solar intensity, as seen by the stationary pyrheliometer, was generally a parabolic curve peaking at solar noon to 0.59 solar constant; and the heat gain curve was a nonsymmetrical parabolic shape with its peak some 15 to 20 min later than solar noon. This considerable time lag and the deviation from a symmetrical curve were undoubtedly due to the thermal inertia of the relatively heavy collector plate. The sealed tube collector plate weight was not measured prior to the time it was sealed inside the glass tube, so its exact weight is not available. However, the plate was made from 2.381 mm (0.09375 in.) copper stock. Using the 0.081 m$^2$ plate area at a thickness of 2.381 mm and the specific gravity of copper (8.94), an approximate weight of the copper plate can be calculated. Calculations indicated the approximate weight of the plate was 1.73 kg (3.814 lb), excluding the weight of the tubing. Another piece of tubing of the same wall thickness and approximately the same length was obtained and weighed. Its weight was found to be 258.2 grams (0.569 lb); therefore, the total weight of the plate tested must have been approximately 1.988 kg (4.383 lb). The intent had not been to assemble a heavy collector but to make one from available material. At the time the plate was made the intent was to run all tests at steady state conditions, so the thermal mass of the plate would not have been a serious concern. This particular test was added to the plan as the outdoor series was being performed.

Since there was some data scatter, the curves shown for solar intensity and for heat gain are an average of the plotted data taken every 10 min. The heat gain data scatter was approximately 0 to ±9.65 × 10$^4$ J/m$^2$/h (0 to ±8.5 Btu/ft$^2$/h) off the nominal curve shown. The average solar intensity curve
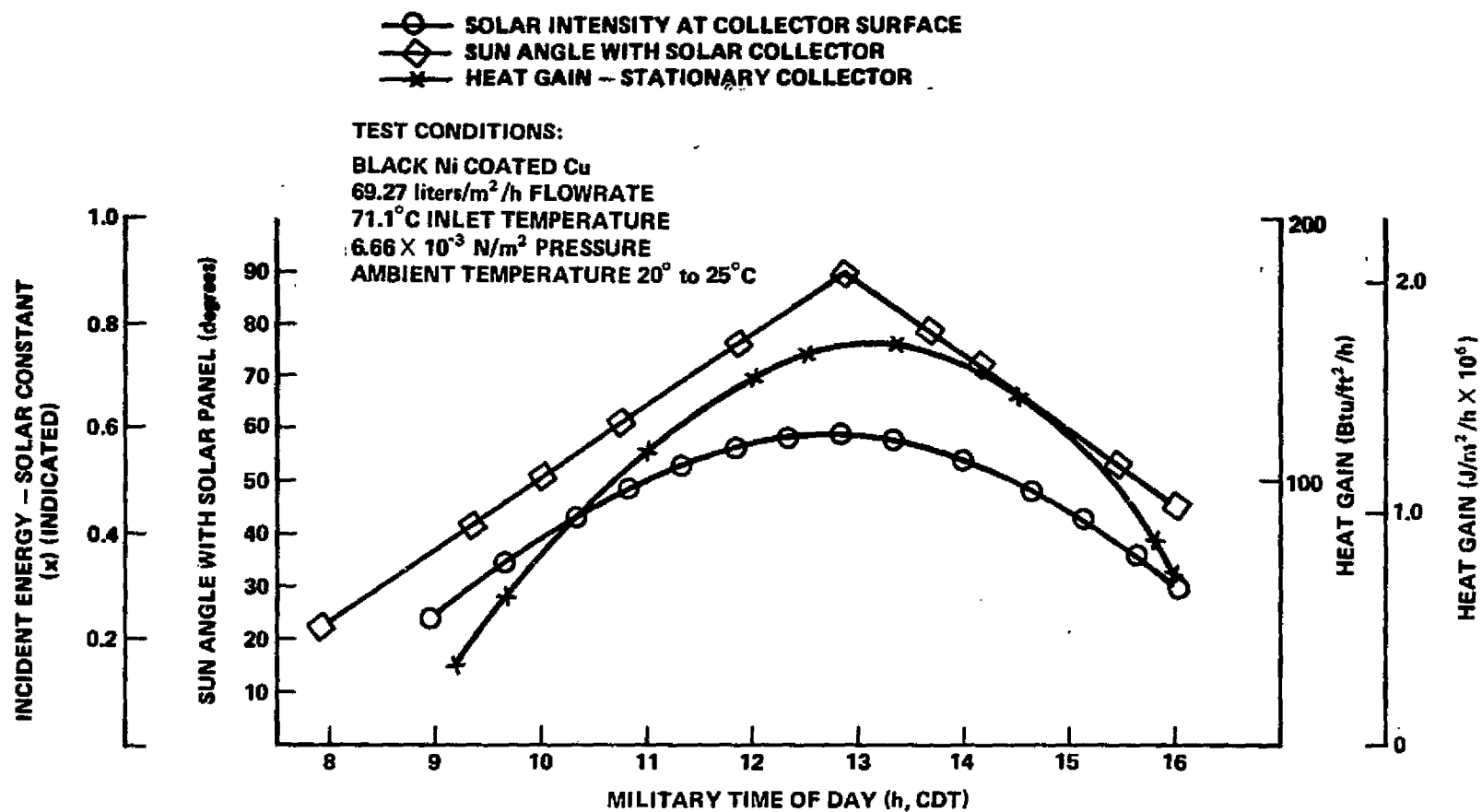
Figure 34. Solar intensity, Sun angle, and heat gain versus time (0.081 m² sealed tube evacuated collector).

shown was drawn using data points from 0 to ±0.015 solar constant off nominal. It should be noted that the heat gain curve shown reflects an energy conversion utilizing only the front side of the solar panel. Black paper was placed under the glass tube to minimize reflection from the plywood mounting board to the backside of the collector plate.

4. **Comparison of the Heat Gain as a Function of Inlet Temperature Performance of Two Different Vacuum Tube Sizes.** The purpose of Figure 35 was to compare the data taken from tests of the two different sizes of vacuum tube collectors tested, as discussed previously. The data plotted in both cases were from black nickel coated copper collector plate tests. The primary differences between the two collectors and test conditions concerned the size of the collector plate being tested and the solar source. The solar simulator was used in the test of the smaller collector $(0.01579 \text{ m}^2)$, whereas the larger collector $(0.081 \text{ m}^2)$ was tested in sunlight. The performance of both units tended to converge at approximately 20°C (68°F), if the lower curve is extrapolated to the left. It can also be noted that their performance diverges considerably at the high inlet temperature end of the curve. The decrease in heat gain performance with increasing inlet temperature of the smaller collector is the result of conductive heat losses through the water flow tubing, which are an appreciable percentage of the total heat gain involved. Conductive heat losses of a similar magnitude on the larger solar collector would be a smaller percentage of the total heat gain involved; consequently, the decrease in performance would be less apparent at the higher inlet temperatures. This aspect of "scaled-down" testing would indicate that there is a practical limit to "scaling down" solar collectors for testing and evaluation and that limited larger scale tests should be made to verify results.

# VI.  CONCLUSIONS

The modular solar collector test system is a convenient test device. In conjunction with a solar simulator, scaled-down solar collector systems or solar collector coatings can be tested and evaluated rather easily, as compared to full scale tests conducted in sunlight. Carefully controlled tests using solar simulation can provide useful comparative data that are more economically, easily, and readily obtained than outdoor test data. However, there are some cautions that should be observed. Data indicate that there is a useful limit

**TEST CONDITIONS:**

BLACK Ni COATING ON Cu
0.75 SOLAR CONSTANT
69.27 liters/m$^2$/h FLOWRATE
1.333 X 10$^{-2}$ N/m$^2$ PRESSURE

$\alpha$ = 0.87, $\epsilon$ = 0.05
AMBIENT TEMPERATURE 16°C

$\alpha$ = 0.79, $\epsilon$ = 0.05
AMBIENT TEMPERATURE 25°C

—△— 0.081 m$^2$ VACUUM TUBE
DIRECT SUNLIGHT SOURCE, NORMALIZED
—○— 0.01579 m$^2$ VACUUM TUBE
SOLAR SIMULATOR SOURCE

HEAT GAIN (J/m$^2$/h X 10$^6$)

HEAT GAIN (Btu/ft$^2$/h)

EFFICIENCY

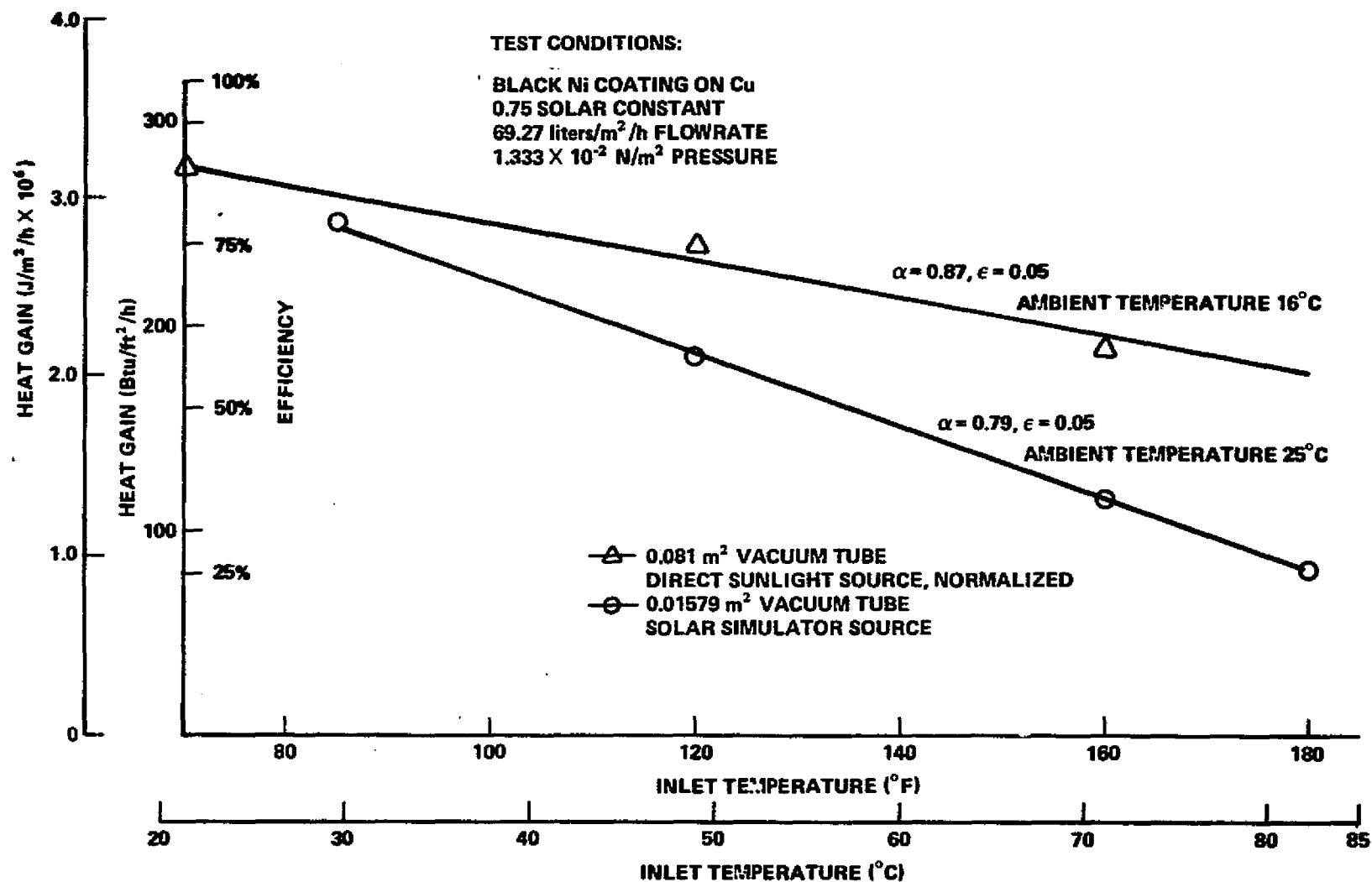INLET TEMPERATURE (°F)

INLET TEMPERATURE (°C)

Figure 35. Heat gain versus inlet temperature for two vacuum tube collector sizes.

beyond which scaled-down testing can produce results which deviate considerably from results of larger scale tests, even when rather extensive precautions are taken to ensure minimum heat losses and accurate results. Experience would indicate that limited larger scale tests and tests in sunlight should be performed to properly model simulation testing.

The data acquisition system and data processing system utilized provided an accurate and convenient data printout with a minimum of time and effort. Large quantities of data were reduced, and hundreds of repetitive calculations were performed easily and quickly by the system. The data printout was compact, simple to use, and easy to store. This type of system is recommended where large amounts of data must be processed.

Vacuum insulated solar collectors tested to date have not been optimized; considerable improvement should be possible. Optimized units with concentrating reflectors should permit operating temperatures high enough for use in absorption air conditioning systems.

The insulated box collector with a nonselective coating such as Caldwell No. 129-386 flat black paint performed very well, within the temperature limits of these tests. With this type of collector and within the temperature limits of these tests, a coating's absorptivity tended to be the controlling factor in its heat gain performance; the coating's emissivity appeared to be a less important factor. The emissivity would become an increasingly important factor at higher collector temperatures. These tests show that a low cost nonselective coating would be sufficient in a collector of this type for space heating and service hot water systems.

Since the test setup utilized a closed loop water system with a reservoir, the reservoir temperature normally rose during a test run. The magnitude of the temperature rise was dependent on several factors including the size of the solar collector, the water flow rate, the amount of auxiliary heat required to maintain a steady state inlet temperature, the quantity of water in the system, and the duration of the test. This temperature rise caused a change in water density and viscosity that resulted in a gradual change in water flow rate through the needle-type water flow control valve. This system temperature rise also caused a need for a gradual decrease in auxiliary heat to maintain a constant inlet temperature to a collector. The above characteristics made it necessary to monitor the water flow rate and inlet temperature to the collector under test,

71

and to make occasional small adjustments to flow rate and auxiliary heat to assure that steady state conditions were maintained at the inlet of the collector under test. During the test program it became apparent that automatic control of these parameters would be a desirable feature, or that a heat exchanger might be added to remove heat from the system at a variable and controllable rate such that reservoir and system temperature could be held constant and occasional small adjustments to water flow rate and auxiliary heat would not be necessary. Efforts are being made to modify the test setup such that its operation will be automatic.

In the past, solar collector panel coating absorptivity and emissivity measurements were made at $37.78^{\circ}C$ ($100^{\circ}F$) by the Ceramics and Coatings Branch, Materials and Processes Laboratory, MSFC. New equipment has been ordered and is being installed which will permit these measurements to be made from room temperature to $760^{\circ}C$ ($1400^{\circ}F$). This will permit more thorough and complete characterization of the coatings being evaluated.

Current plans are to continue testing scaled-down solar collector systems.

# APPENDIX

# LIST OF EQUIPMENT USED IN THE TEST PROGRAM

1. Water Circulation System — Test Bed

   a. Pump, Eastern Industries, model F 346, type 1068; drive motor, General Electric, model 5KN23 AC 304, 115 V, 1 phase, 1725 rpm

   b. Reservoir, 9 gal, CRES steel sphere, 200 psi pressure rated

   c. Filter, Fluid Dynamics, P/N FR 1564-4006, 40 $\mu$m

   d. Flow control valve, Nupro, model 4BMW, needle throttling micrometer type

   e. Flowmeter, Flow Scan Instrument Company, series 300

   f. Heater, model LIE24, Watlow, St. Louis, MO

   g. Heater housing, 304 CRES, locally fabricated

   h. Relief valve, Republic Manufacturing Co., P/N 647-3-6

   i. Check valve, Republic Manufacturing Co., P/N 418-4

   j. Hand valve, pump inlet, 3/8 in., 304 CRES, Robbins Aviation Inc.

   k. Hand valves, system pressurizing and water level shutoff, 1/4 in., 304 CRES, Robbins Aviation Inc., two each

   l. Hand valve, fill and drain, 1/2 in., 304 CRES, Robbins Aviation Inc.

   m. Pressure gauge, reservoir, pump inlet, pump outlet, 0 to 100 psig, Robertshaw Accraguage, three each

n. Pressure gauge, test panel inlet and outlet, 0 to 60 psig, U. S. Gauge, two each.

o. Pressure transducer, reservoir, ALINCO (Allegheny Instrument Co.), model HAC 118, S/N 40994, 50 psig

p. Pressure transducer, pump discharge and test panel inlet, ALINCO, model HAC 118, S/N's 41090 and 41141, 100 psig

q. Pressure transducer, test panel differential pressure, Statham Instruments, model PM 280, S/N 3416, 10 psid

r. Tube, water level sight, clear Tygon plastic, 1/4 in. bore

s. Transformer, toroidal heater voltage control, adjustable, General Electric, model 9T 92Y7

t. Thermocouples, chromel-alumel, calibrated

2. Vacuum Test Equipment

a. Thermocouple gauge control, model TG-7, S/N 00-5882, Veeco Instruments, Plainview, NY

b. Cryosorb cold trap, 4 in., series 250-4, Granville Phillips Co.

c. Oil diffusion pump, 4 in., catalog No. 93405, Cenco, Central Scientific Division, Cenco Instruments Corp.

d. Mechanical vacuum pump, model 1397, S/N 25108, The Welch Scientific Co., Skokie, IL

e. Digital ionization gauge control, model 605-0019, S/N 9762, Perkin Elmer-Ultek, Mountain View, CA

f. Dewar, 76 liter liquid nitrogen storage, Union Carbide, model LS-160, Department of Transportation No. 4L150

g. Valve, solenoid, liquid nitrogen shutoff, ASCO valve catalog No. 8263A207LT, solenoid catalog No. 80034, 120 V, 60 Hz, Automatic Switch Co., Florham Park, NJ

h. Time switch, Tork, model 4100 Hourmaster Series, 120 V, 60 Hz, Tork Time Controls, Mount Vernon, NY

3. Data Acquisition System

a. Voltmeter, integrating digital, model 2401C, Hewlett Packard, Palo Alto, CA

b. Scanner, input, model 2901A, Hewlett Packard, Palo Alto, CA

c. Coupler, timer, model 2547A, Hewlett Packard, Palo Alto, CA

d. Counter, preset, model 5214L, Hewlett Packard, Palo Alto, CA

e. Oscilloscope, storage, type 549, Tektronix Inc., Portland, OR

f. Teletype, model 2752A, Hewlett Packard, Palo Alto, CA

g. Pyrheliometer, model P-8400-B, Hy-Cal Engineering, Santa Fe Springs, CA

h. Recorder, strip chart, two channel, model 7100B with model 17501A amplifiers, Hewlett Packard, Palo Alto, CA

i. Multimeter, digital, model 3469B, Hewlett Packard, Palo Alto, CA

4. Data Reduction System

a. Tape reader, high speed photo, model 2748A, Hewlett Packard, Palo Alto, CA

b. Computer, model 2116C, Hewlett Packard, Palo Alto, CA

c. Teletype, model 2752A, Hewlett Packard, Palo Alto, CA

5. Solar Simulator — 6 kW xenon tube type, noncollimated, variable intensity, locally assembled from parts

6. Spectroradiometer — model SR, S/N 2063, Instrumentation Specialities Co., Inc., Lincoln, NE

# REFERENCES

1.  Koller, Lewis R.: Ultraviolet Radiation. John Wiley & Sons, New York, 1965.

2.  Krider, Jan F. and Kreith, Frank: Solar Heating and Cooling. Scripta Book Company, Division of Hemisphere Publishing Corp., Washington, D.C., 1975.
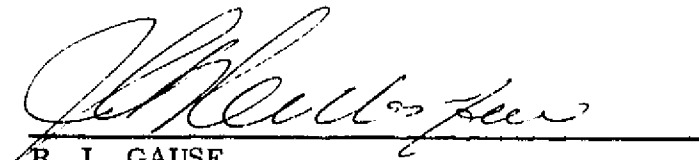
76

# APPROVAL

# A PERFORMANCE EVALUATION OF VARIOUS COATINGS, SUBSTRATE MATERIALS, AND SOLAR COLLECTOR SYSTEMS
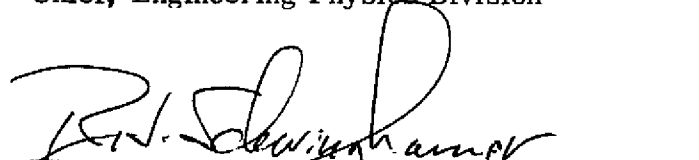
By F. J. Dolan

The information in this report has been reviewed for security classification. Review of any information concerning Department of Defense or Atomic Energy Commission programs has been made by the MSFC Security Classification Officer. This report, in its entirety, has been determined to be unclassified.

This document has also been reviewed and approved for technical accuracy.

R. L. GAUSE
Chief, Engineering Physics Division

R. J. SCHWINGHAMER
Director, Materials and Processes Laboratory